SEQUENCE STRATIGRAPHY OF THE NEOPROTEROZOIC INFRA KROL FORMATION AND KROL GROUP, LESSER HIMALAYA, INDIA

GANQING JIANG[1], NICHOLAS CHRISTIE-BLICK[1], ALAN J. KAUFMAN[2], DHIRAJ M. BANERJEE[3], AND VIBHUTI RAI[4]
[1] *Department of Earth and Environmental Sciences and Lamont-Doherty Earth Observatory of Columbia University, Palisades, New York 10964–8000, U.S.A.*
[2] *Department of Geology, University of Maryland, College Park, Maryland 20742–4211, U.S.A.*
[3] *Department of Geology, University of Delhi, Delhi 110007, India*
[4] *Department of Geology, Lucknow University, Lucknow 226007, India*
e-mail: ganqing@ldeo.columbia.edu

ABSTRACT: **A sequence stratigraphic study of terrigenous and carbonate rocks of the Infra Krol Formation and Krol Group in the Lesser Himalaya fold and thrust belt of northern India was undertaken as part of a broader investigation of the significance of carbon isotope data in Neoproterozoic successions. Eight regional stratigraphic discontinuities were traced over a distance of nearly 300 km, and interpretations were anchored in a series of local studies involving the mapping of key beds and the measurement of closely spaced sections. Three of the regional surfaces are interpreted as sequence boundaries on the basis of (1) locally developed incised valleys < 60 m deep; (2) paleokarstic depressions with < 50 m of mappable relief; (3) subaerial dissolution and weathering products (breccias and calcrete) filling vertical fissures, dikes, cavities, and shallow depressions in underlying carbonate rocks; and (4) small-scale evidence for subaerial exposure at an erosion surface. The remaining five discontinuities are regional flooding surfaces identified on the basis of either facies changes with an abrupt upward deepening across the surface or transitions in facies stacking patterns, typically from forestepping to backstepping. A glacio-eustatic origin is permitted, although not required, for the three sequence boundaries, but no evidence has been found for marked lowering of sea level at other horizons. A mismatch between the stratigraphic location of sequence boundaries and carbon isotope minima suggests that local diagenetic alteration or oceanographic phenomena unrelated to glaciation may be in part responsible for observed isotopic variation, and that small ice sheets may have existed during apparently nonglacial times without producing either cap carbonates or negative carbon isotope excursions.**

INTRODUCTION

The span of Earth history encompassing the final 200 m.y. of the Neoproterozoic, from ~ 750–543 Ma, is one of the most remarkable in the evolution of our planet owing to unusually widespread glaciation (Harland 1964; Kirschvink 1992; Hoffman et al. 1998; Crowell 1999; Sohl et al. 1999; Evans 2000), and to the emergence, for the first time in the patchy fossil record, of macroscopic animals (Knoll and Walter 1992; Grotzinger et al. 1995; Bowring and Erwin 1998; Xiao et al. 1998; Knoll 2000). An approach that has proven particularly useful in studying this geology is carbon isotope chemostratigraphy, both as a monitor of paleoenvironmental change and as a tool for global correlation (Knoll et al. 1986; Narbonne et al. 1994; Kaufman and Knoll 1995; Pelechaty et al. 1996; Kaufman et al. 1997; Saylor et al. 1998; Jacobsen and Kaufman 1999; Knoll 2000). However, questions remain about the completeness of the isotopic record in successions with only sporadic development of carbonate rocks, about how that record may have been modified by diagenesis, and about the potential circularity inherent in correlating curves from different locations in the absence of adequate independent chronology.

It is in this context that we undertook a sequence stratigraphic study of the Neoproterozoic Infra Krol Formation and Krol Group in the Lesser Himalaya fold and thrust belt of northern India. Shallow-marine carbonate rocks amenable to chemostratigraphic analysis are unusually abundant in the Krol Group (< 1400 m thick in sections that we have measured, and < 2050 m according to Shanker et al. 1993 and Shanker et al. 1997), and the tracing of physical surfaces offers a way of establishing relative ages in different sections independently of geochemical data (Christie-Blick and Driscoll 1995). Sequence boundaries and other stratigraphic discontinuities are recognized at several levels in both the Infra Krol and Krol, although their expression is mostly subtle. This is attributed in part to local factors influencing the development of karst. Our data nevertheless place constraints on the amplitude of any glacially induced sea-level changes during the span of time represented by the Infra Krol and Krol, and on competing schemes for the global correlation of Neoproterozoic glacial rocks (Kaufman et al. 1997; Kennedy et al. 1998; Saylor et al. 1998; Knoll 2000). Details of our chemostratigraphic studies will be published elsewhere.

GEOLOGICAL FRAMEWORK

The Infra Krol Formation and Krol Group are part of a Neoproterozoic and Lower Cambrian succession more than 12 km thick, cropping out in the Lesser Himalaya in a series of doubly plunging synclines between Solan in the northwest and Nainital, 280 km to the southeast (Fig. 1; Bhargava 1979; Shanker et al. 1989; Shanker et al. 1993; Shanker et al. 1997; Shanker and Mathur 1992). The lower half of this succession consists of quartzite, sandstone, argillite, carbonate rocks, and minor mafic volcanic rocks of uncertain age, but younger than 1 Ga, and possibly rift-related (Jaunsar and Simla groups; Singh 1980a; Kumar and Brookfield 1987; Shanker et al. 1989). The upper half of the succession begins at an unconformable contact with as much as 2 km of diamictite, siltstone, and sandstone of glacial and glacial-marine origin (Blaini Formation in Fig. 2; Bhatia and Prasad 1975; Gupta and Kanwar 1981; cf. Singh 1980a for a different view). These rocks are overlain by a ''cap carbonate'' no more than a few meters thick (uppermost Blaini), and by up to 400 m of shale, siltstone, and minor sandstone assigned to the Infra Krol Formation. Carbonate rocks of the overlying Krol Group are overlain in turn by as much as 2800 m of mostly terrigenous rocks of Cambrian age (Tal Group), with a distinctive unit of black shale, chert, and phosphorite up to 150 m thick at the base.

These younger Neoproterozoic and Cambrian rocks are interpreted to represent the inner part of a north-facing passive continental margin (Brookfield 1993), with a rift to post-rift transition tentatively interpreted within or perhaps at the base of the Blaini. A passive-margin setting is inferred on the basis of scale, the absence of igneous rocks, and comparatively simple regional facies and thickness trends within the Infra Krol and Krol, with no evidence for the syndepositional tectonism that might be expected in a foreland basin (e.g., Plint et al. 1993; Yang and Dorobek 1995). Neoproterozoic(?) to Middle Cambrian strata are exposed to the north in the High Himalaya, but the tectonic and stratigraphic relations of these rocks with respect to the Lesser Himalayan succession are unknown. The rocks of the High Himalaya represent either a continuation of the northern passive margin of the Indian craton or an unrelated succession that was accreted to the Indian continent during the early Paleozoic (DeCelles et al. 2000). The High Himalaya contains evidence for early Ordovician deformation, metamorphism, and granite intrusion that together signal a tectonic event (Le Fort et al. 1983; Garzanti et al. 1986). Any stratigraphic evidence for such an event, if it affected the Lesser Himalaya, would have been removed by erosion beneath a profound pre-Permian unconformity. The Cambrian Tal Group of the Lesser Himalaya is directly overlain by a comparatively thin carapace of Permian and Cretaceous strata. All of the rocks were thrust southwestward as a result of the India–Eurasia collision, beginning approximately 55 m.y. ago (Powers et al. 1998; Hodges 2000). Deformation on the Main Boundary thrust, which structurally underlies the Lesser Himalaya, began prior to 10 Ma, and continues today (Valdiya 1992).

Prior Work and Lithostratigraphy of the Infra Krol–Krol Interval

Previous studies of the Infra Krol–Krol interval have dealt mainly with regional lithostratigraphy and paleontology (e.g., Singh 1980a, 1981; Singh and Rai 1983; Shanker et al. 1989; Shanker and Mathur 1992; Shanker et al. 1993). Sedimentological studies have focused primarily on portions of the stratigraphy with features ascribed to tidal and tidal-flat environments: microbial laminae, fenestral structure, gypsum casts, and desiccation cracks (Singh 1980a, 1980b; Singh and Rai 1980; Singh et al. 1980; Misra 1984).

The most widely used regional stratigraphic terminology for the interval of interest is based on an informal scheme proposed by Auden (1934) in the vicinity of Solan (Figs. 1, 2), including the Infra Krol, Krol Sandstone, Lower Krol (Krol A), Middle Krol (Krol B), and Upper Krol (Krol C, D, and E). Shanker et al. (1993) and Shanker et al. (1997) recommended raising the Krol to group status and formalizing internal subdivisions as Chambaghat Formation (Krol Sandstone), Mahi Formation (Krol A), Jarashi Formation (Krol B), and Kauriyala Formation (Krol C, D, and E). These are shown in Figure 2, although informal letter designations are

JOURNAL OF SEDIMENTARY RESEARCH, VOL. 72, NO. 4, JULY, 2002, P. 524–542
 1527-1404/02/072-524/$03.00

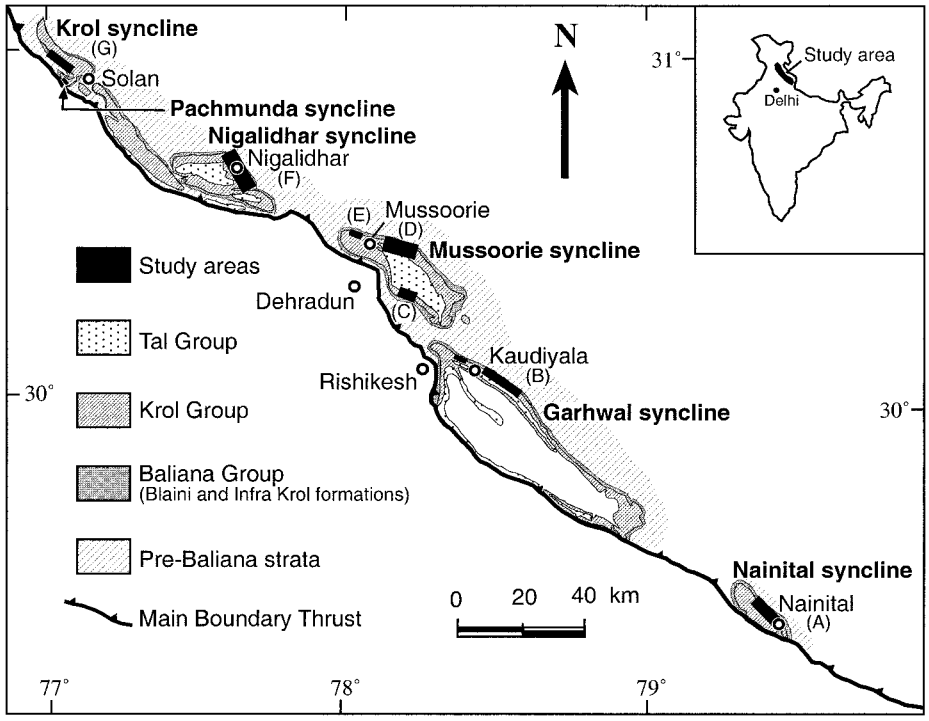

FIG. 1.—Geological map showing exposures of Neoproterozoic strata in Lesser Himalaya fold and thrust belt (modified from Singh and Rai 1983; Shanker et al. 1997). Letters A to G indicate location of representative sections in study areas (see Figs. 3 and 4).

retained in this paper for the sake of simplicity, and because they are still widely used by Indian geologists.

The Krol A consists of argillaceous limestone interbedded with greenish-gray calcareous shale. Krol B is characterized by a distinctive grayish-red shale and siltstone with thin, lenticular beds of dolomite. Krol C is composed of bluish-gray crystalline limestone and dark gray dolomitic limestone, in places brecciated and containing fenestral structure. Krol D is represented by dolomitic limestone, microbial cherty dolomite, calcareous shale, siltstone, and minor sandstone. Krol E consists of limestone interbedded with calcareous shale, siltstone, argillaceous limestone, and dolomite. Krol units A, B, and E, and the green to gray shale of the underlying Infra Krol Formation, can be recognized and confidently mapped throughout the Lesser Himalaya. However, Krol units C and D are of more variable lithology and thickness (Shanker and Mathur 1992; Shanker et al. 1993), and they are less easily distinguished. We have followed the common Indian practice of locating the lithostratigraphic boundary between these units on the basis of the greater abundance of shale and siltstone in Krol D. The Krol Sandstone is a distinctive coarse- to fine-grained quartz sandstone with abundant cross-stratification. Unlike the other stratigraphic units, it is restricted mostly to the area near Solan (Fig. 1), although we have recognized a similar sandstone at the same stratigraphic level in the vicinity of Nainital.

Paleontological and Chemostratigraphic Evidence for Age

No radiometric age data are available for the Infra Krol–Krol interval. It is generally assigned a terminal Proterozoic age by Indian geologists on the basis of (1) close lithostratigraphic similarities with the postglacial Neoproterozoic and Cambrian succession of southern China; (2) assemblages of small shelly fossils of Cambrian age (possibly early Tommotian or equivalent to the Meishucunian of southern China) reported from chert–phosphorite of the basal Tal Group (Azmi 1983; Rai and Singh 1983; Bhatt et al. 1985; Brasier and Singh 1987; Kumar et al. 1987; Bhatt 1989, 1991); (3) small acanthomorph acritarchs of late Nemakit–Daldynian affinity recovered from the same interval (Tiwari 1999); (4) ''Ediacaran'' impressions reported in Krol D and Krol E carbonates and siltstones (Mathur and Shanker 1989, 1990; Shanker and Mathur 1992; Shanker et al. 1997), and possible remains of Ediacaran metaphytes in Krol A carbonates (Tewari 1993a); (5) possible simple trace fossils from the upper part of Krol D and Krol E (Singh and Rai 1983); and (6) abundant cyanobacterial filaments, coccoids, acanthomorph acritarchs, and vase-shaped microfossils reported from chert nodules in Krol A (Kumar and Rai 1992; Tiwari and Knoll 1994; Gautam and Rai 1997). Other fossils reported from the Krol Group, such as algae (Singh and Rai 1983; Mathur 1989) and stromatolites (Singh and Rai 1977, 1983; Tewari 1993b; Tewari and Joshi 1993), are of lesser age significance.

The precise location of the Precambrian–Cambrian boundary has been questioned on both paleontological and chemostratigraphic grounds. The lithostratigraphic contact between the Krol and Tal groups is located with difficulty in some sections, and, as locally mapped, it does not necessarily correlate precisely with the marine flooding surface that commonly marks the boundary (surface 8 in Fig. 2). However, a report of small shelly fossils from the Krol D level at Mussoorie syncline (Azmi and Pancholi 1983) was discounted by Bhatt (1991) as misinterpretation of a structural slice of Tal Group within the Krol. The supposed Ediacaran fossils in Krol D and Krol E are also problematic because they are poorly preserved and not necessarily of biological origin. Attempts to find additional specimens at the original sampling sites have proven unsuccessful (Misra 1990, 1992; Bhatt 1996). In the absence of firm paleontological control, Knoll et al. (1995) and Kaufman and Knoll (1995) suggested that the Cambrian might encompass strata as low as Krol C, on the basis of sparse published carbon isotope data (Aharon et al. 1987). That interpretation was tentative, however, given the very coarse sampling ($>$ 50 m) of the chemostratigraphy that was available at the time. Banerjee et al. (1997) studied geochemical changes across the Krol E–Tal transition in some detail, and assigned the Krol E to the Nemakit–Daldynian (basal Cambrian) on the basis of a carbon isotope maximum ($\delta^{13}C \sim 0‰$) in the upper part of Krol E and an abrupt change to negative values in the Tal. However, our most recent studies cast doubt on the existence of the maximum. The absence of fossils of clear Cambrian affinity in the Krol suggests that it is entirely of Neoproterozoic age, with a portion of the Nemakit–Daldynian (543–530 Ma; Bowring and Erwin 1998) possibly missing at the Krol–Tal contact, along with an indeterminate part of the Proterozoic. The latter may include the span of an inferred short-lived latest Proterozoic negative carbon isotope excursion ($<$ 1 m.y.; Grotzinger et al. 1995) for which there is no record in the Lesser Himalaya.

LITHOFACIES, FACIES ASSOCIATIONS, AND PLATFORM MORPHOLOGY

Eighteen lithofacies have been identified in the Infra Krol Formation and Krol Group on the basis of composition, grain types, sedimentary structures, diagenesis, and vertical facies relationships. These lithofacies are grouped into eight genetically significant facies associations. The lithology, major sedimentary structures, and environmental interpretations of facies and facies associations are summarized in Table 1 and in Figures 3 and 4.

Facies of the Infra Krol and lower and upper parts of the Krol are comparatively simple, with shoaling-upward trends characterizing sections from each syncline. These typically consist of upward transitions from shale and mixed shale–limestone to more massive carbonate rocks including microbial dolomite (Figs. 3, 4).

The middle Krol displays greater facies variability, with an outer shelf marked by a stromatolite-rich peritidal carbonate complex that may have served as a barrier

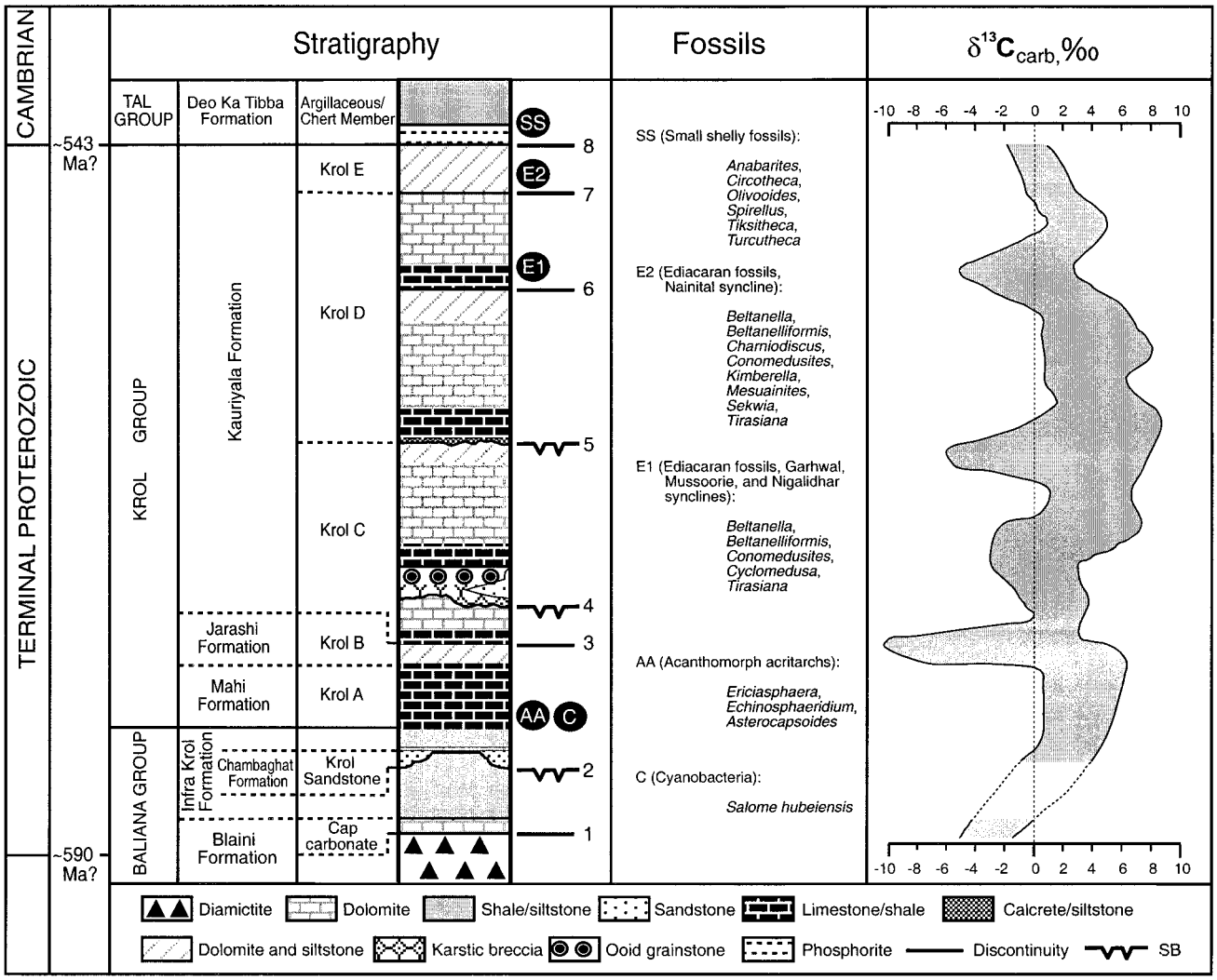

FIG. 2.—Generalized stratigraphy of Infra Krol Formation and Krol Group showing stratigraphic nomenclature, reported fossil discoveries, interpreted sequence boundaries (SB), and other regional stratigraphic discontinuities, and a compilation of carbon isotope data (864 samples from 25 sections; see Jiang 2002). Details of carbon isotope data will be published elsewhere. Paleontological interpretations are as follows: cyanobacteria (C) and acanthomorph acritarchs (AA) from Tiwari and Knoll (1994); Ediacaran fossils in Krol D (E1) from Shanker et al. (1997); Ediacaran fossils in Krol E (E2) from Mathur and Shanker (1989, 1990) and Shanker et al. (1997); and small shelly fossils (SS) from Kumar et al. (1987) and Bhatt (1991). Only the uppermost part of the Blaini Formation is shown, and the ''cap carbonate'' (5–15 m thick) is exaggerated.

(cf. Sami and James 1994). Stromatolites in this complex vary in shape and size (Table 1). Ooids, peloids, intraclasts, stromaclasts, and oncoids are abundant particles. The peritidal carbonate complex displays an overall shoaling-upward trend, expressed by an upward increase of shallow-water features such as small-scale wave ripples, microbial laminae, fenestrae, vugs, tepees, pedogenic pisolites, desiccation cracks, and exposure-related brecciation. Lagoonal facies are comparatively fine-grained, with abundant organic-rich shale and wackestone.

The relation between the outer-shelf, lagoonal, and inner-shelf facies associations has been documented at Nigalidhar syncline for the interval between surfaces 4 and 5 (section F in Figs. 3 and 4; Fig. 5). At any location, lagoonal facies alternate with stromatolitic dolomite of the peritidal carbonate complex (outer shelf), and they pass upward into peritidal carbonate–siliciclastic facies containing abundant shallow-water features (inner shelf). Outer-shelf rocks become more abundant towards the north at Nigalidhar syncline, and they pass laterally into lagoonal and inner-shelf facies along the Lesser Himalaya towards the southeast. This platform architecture (Fig. 6A) is comparable to that of several well known Paleoproterozoic examples: the Pethei and Rocknest platforms of northwest Canada (Grotzinger 1986a, 1986b, 1989; Sami and James 1993, 1994) and the Transvaal Supergroup of southern Africa (Beukes 1987). In the case of the Krol, however, the outermost rim and slope are not preserved in outcrop.

SEQUENCE STRATIGRAPHY

Standard concepts and methods of sequence stratigraphy (Vail 1987; Van Wagoner et al. 1990; Sarg 1988; Handford and Loucks 1993; Posamentier and James 1993; Christie-Blick et al. 1995; Christie-Blick and Driscoll 1995) have been applied to the Infra Krol Formation and Krol Group. Central to this approach is the lateral tracing of physical surfaces. This was achieved initially in small areas by the mapping of key beds and the measurement of closely spaced sections, with emerging patterns gradually extended to adjacent areas within the same syncline, and eventually from one syncline to another. The scale of the Lesser Himalaya, structural complexities, landsliding on steep slopes, and locally dense vegetation preclude the tracing of any surface continuously through the outcrop belt. However, detailed work provides convincing evidence for the interpretation of three prominent sequence boundaries (surfaces 2, 4, and 5 in Fig. 3). These and five additional stratigraphic discontinuities can be confidently recognized in each of five synclines that we have studied.

The eight regional discontinuities are identified and correlated on the basis of (1) a transition in facies stacking patterns, typically from a forestepping motif (from subtidal dominated units to intertidal–supratidal dominated units) to a backstepping motif (from intertidal dominated units to subtidal dominated units; e.g., Fig. 6B); (2) abrupt facies changes in individual sections; and (3) regional facies architecture.

TABLE 1.—*Summary of facies and facies associations.*

Lithofacies	Constituents	Bedding and structures	Interpretation
DEEP SUBTIDAL			
Calcareous shale and siltstone	Gray to green calcareous shale and siltstone; rare very fine-grained sandstone	Laterally continuous, millimeter-thick parallel lamination; small-scale wavy cross-lamination in sandstone layers; commonly as monotonous, noncyclic intervals	Deep subtidal below fair-weather wave base
Mixed shale and limestone	Unevenly interbedded calcareous shale-siltstone and lime mudstone–wackestone; rare fine-grained peloidal grainstone	Laterally continuous, millimeter-thick parallel lamination; rare wavy cross-lamination with minor erosional surfaces; grainstone layers; shale–limestone alternation	Deep subtidal, occasionally shallowing to wave base
Muddy dolomite	Greenish to gray muddy dolomite; locally interbedded with millimeter-scale fissile shale	Thin-bedded; parallel lamination	Deep subtidal below fair-weather wave base
SHALLOW SUBTIDAL			
Dolograinstone–packstone–shale	Fine-grained oolitic, peloidal grainstone layers and lenses unevenly interbedded with calcareous shale; rare intraclastic grainstone–packstone layers or lenses	Grainstone–packstone: lenticular layers with minor erosional surfaces against shale; small-scale cross-lamination; rare normal graded bedding Shale: thin bedded; parallel lamination	Shallow subtidal at times wave-influenced
Dolopackstone–wackestone–siltstone	Fine-grained peloidal, silty dolopackstone–wackestone interbedded with gray calcareous siltstone	Laterally continuous bedding; wave ripples and small-scale cross-lamination in both siltstone and carbonate layers	Shallow subtidal above fair-weather wave base
SAND SHOAL			
Oolitic–peloidal grainstone	Fine- to coarse-grained oolitic, peloidal grainstone; well-sorted and rounded ooids; rare intraclasts and wavy microbial laminae	Abundant large-scale cross-bedding and small-scale cross-lamination	Shallow subtidal shoal
PERITIDAL CARBONATE COMPLEX			
Wavy microbial dolomite	Thin microbial laminae interbedded with micritic or lenticular grainstone laminae; laterally linked, low-relief stromatolites; peloids, stromaclasts, ooids, and intraclasts	Millimeter-thick, interbedded, undulating, micritic laminae; clasts preserved in small ripples or as fill between stromatolite heads; wave ripples and flaser bedding	Shallow subtidal to intertidal
Oncoid–intraclastic–dolograinstone–rudstone	Intraclasts typically 0.5–2 cm (up to 5 cm) and oncoids (1–10 cm) with superficial coatings; matrix of lime mudstone and fine-grained peloids, ooids, and intraclasts	Tabular to lenticular, discontinuous beds; commonly associated with microbial, stromatolitic dolomites and thin oolitic grainstone layers; small-scale cross-lamination and ripples	Shallow subtidal to intertidal
Stromatolitic dolomite	Couplets of sparry dolomite and crinkled microbial laminae; lenticular beds of lime mudstone, peloids, intraclasts, oncoids, and ooids between stromatolite heads	Convex to undulatory laminae; laterally discontinuous; abundant stromatolites of varying shapes and size; large domal and columnar stromatolites up to 10 to 80 cm synoptic relief, 1–5 m long, interfingered or associated with low-relief (3–8 cm) stromatolites, and grading upwards into microbial laminae with abundant fenestral structure	Shallow subtidal to supratidal
Fenestral microbial dolomite	Dark, relatively organic-rich laminae interbedded with light-colored, irregular, disrupted beds of fenestral fabric; or thick microbial dolomite layers disrupted by small, discontinuously bedded, spar-filled fenestrae	Irregular to discontinuously bedded lamination; poor to moderate lateral continuity; low-relief domal stromatolites; fenestral structures, vugs, tepee structures, desiccation cracks and brecciation	Upper intertidal to supratidal
LAGOONAL			
Organic-rich wackestone–shale	Black to dark-gray, organic-rich dolopackstone–wackestone unevenly interbedded with shale; small peloids and ooids; cherty lenses	Laterally continuous beds; rare columnar stromatolites; parallel lamination	Deep subtidal to shallow subtidal lagoon
Stromatolitic dolomite	Couplets of sparry dolomite and microbial laminae; mud, micrite and peloids in troughs between stromatolite heads	Laterally discontinuous beds associated with organic-rich limestone and microbial laminae; domal and columnar stromatolites with elongate heads; locally developed, high-relief, domal stromatolites of up to 120 cm high	Shallow subtidal to intertidal lagoon
PERITIDAL SILICICLASTIC-CARBONATE			
Microbial dolomite	Dark, relatively organic-rich laminae disrupted by irregular, spar-filled fenestrae, vugs and small dissolution cavities; low-relief domal and columnar stromatolites; chert lenses	Irregular laminae; poor to moderate lateral continuity; fenestrae, vugs, dissolution cavities, tepees, desiccation cracks, and brecciation	Intertidal to supratidal
Cherty dolomite–siltstone	Uniformly chertified, thick (up to 10 m) or thin (2–15 cm) dolomite layers interbedded with dolomitic siltstone; 5–15% terrigeneous quartz silt or sand grains; centimeter-sized domal stromatolites partly replaced by chert	Laterally continuous; wave ripples; fenestrae, pisolites, desiccation cracks, dissolution cavities, and brecciation	Intertidal to supratidal
Massive sparry dolomite	Massive, thick (>5 m, up to 100 m), light-colored, coarse sparry dolomites; centimeter-sized domal stromatolites and thin microbial laminites; up to 10% well sorted quartz silt and sand grains	Massive units; fenestrae, pisolites, vadose cements, vugs, breccias	Intertidal to supratidal
INCISED-VALLEY FILL			
Siliciclastic sandstone–siltstone	Coarse- to fine-grained sandstone and siltstone forming 5 to 25-m-thick, fining-upward units; discontinuous pebbly sandstone or conglomerate layers or lenses at the base	Laterally discontinuous layers; abundant large-scale cross-bedding and small-scale cross-lamination; current ripples; lateral thickness variation	Fluvial channels with large-scale bedforms and bars; karstic valley fill
KARSTIC FILL			
Karstic breccia	Monomict or polymict with lithology similar to host rocks as well as siltstone, shale, and chert clasts; poorly sorted or unsorted, subangular to angular clasts of varying sizes from <1 cm to 3 m; sandy, silty, and micritic matrix	Thin (<0.5 m) or thick (>2 m, up to 20 m), massive or poorly differentiated lenses or layers of varying thickness; laterally traceable to calcrete; vadose cements around breccias; breccia- and sandstone–siltstone-filled dikes and dissolution cavities extending downward into underlying rocks from 2 m to 50 m	Surface karstification products; karstic depression fills
Calcrete	Buff-colored, massive to faintly laminated layers or lenses of dolomudstone, lime mudstone in siltstone; partly silicified patches, pisolite lenses; relict clasts, chert lenses and breccias	Laterally discontinuous over tens of meters; clotted micritic and floating textures	Subaerial exposure

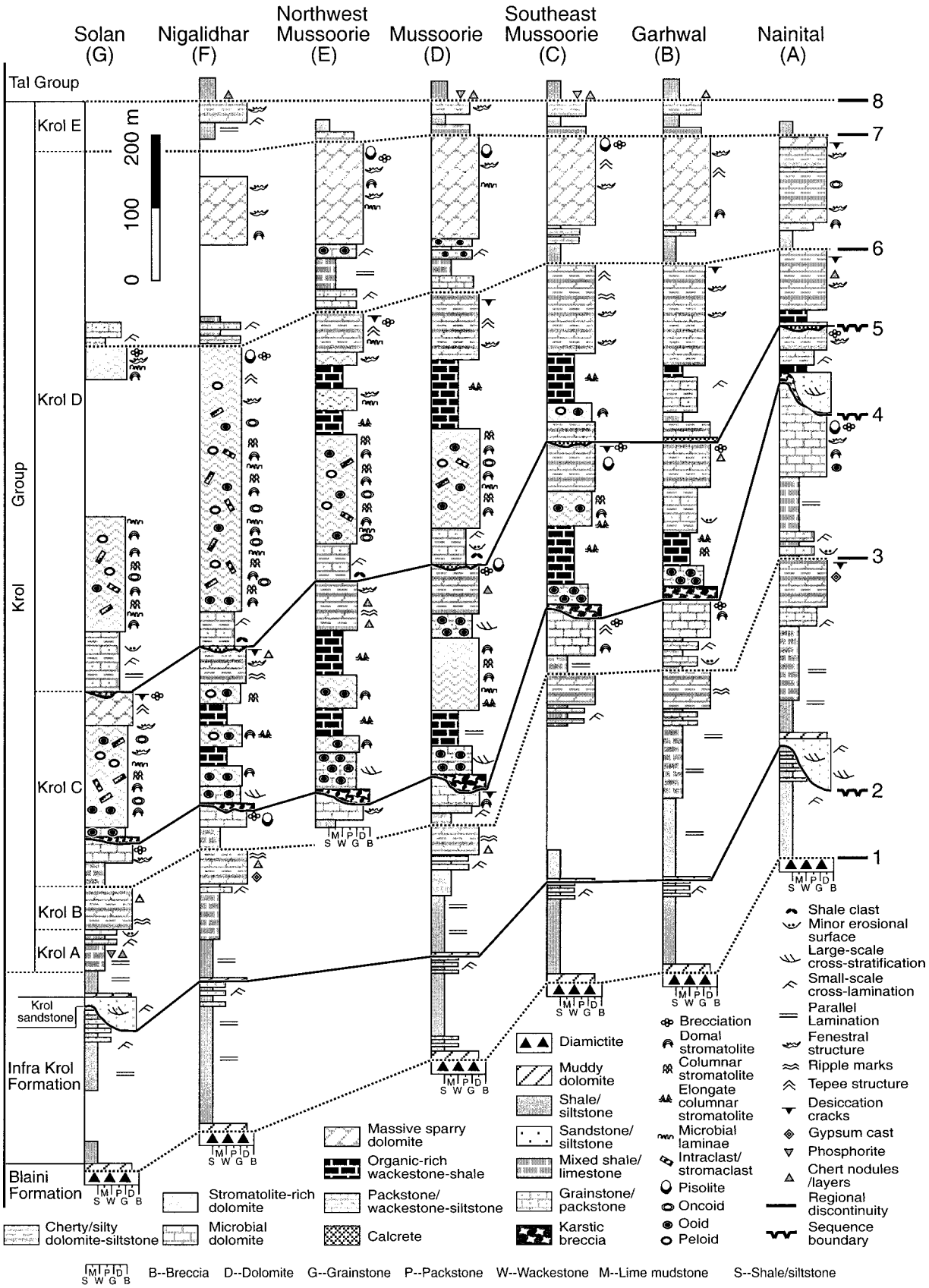

FIG. 3.—Representative stratigraphic sections for Infra Krol Formation and Krol Group, with an interpretation of sequence boundaries and other regional stratigraphic discontinuities. See Figure 1 for locations.

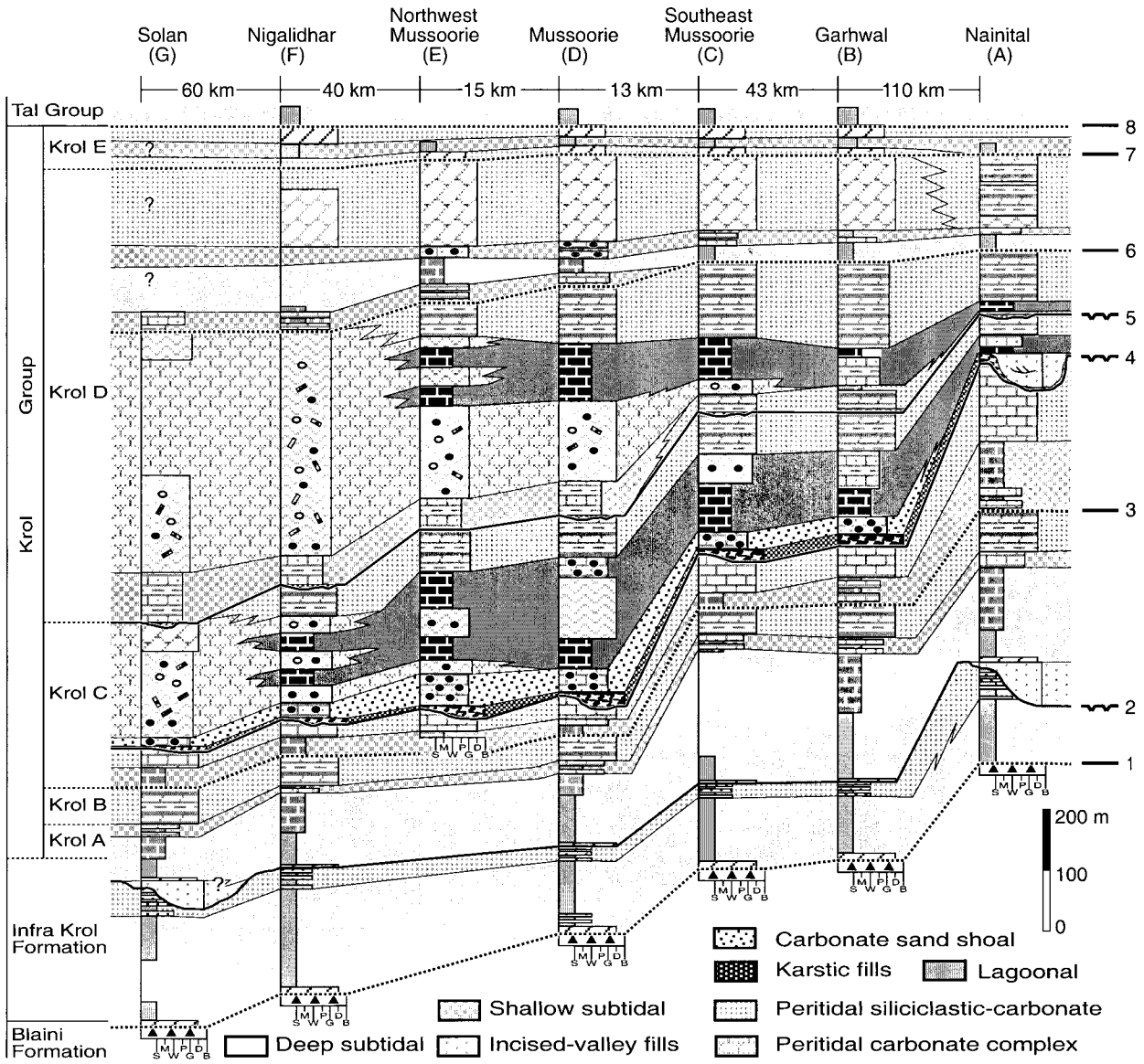

FIG. 4.—Interpretation of facies associations shown in Figure 3 and Table 1.

The sequence boundaries are interpreted with reference to one or more of the following lines of evidence for subaerial degradation: (1) locally developed incised valleys partially filled with siliciclastic sandstone and siltstone; (2) large-scale paleokarstic depressions with mappable relief; (3) subaerial dissolution and weathering products (breccias and calcrete) filling vertical fissures, dikes, cavities, and shallow depressions in underlying carbonate rocks; and (4) small-scale evidence for subaerial exposure at an erosion surface. These features are best displayed in the Nigalidhar, Mussoorie, and Nainital synclines (Figs. 1, 5, 7, 8). In the Solan area (Pachmunda and Krol synclines; Fig. 1), surfaces were traced by means of closely spaced short sections tied to existing geological mapping (Fig. 9). At Garhwal syncline, efforts were focused in the vicinity of the Kaudiyala section (Fig. 1) owing to structural complexities and only sporadic exposure on densely vegetated slopes. Of the five surfaces not clearly interpretable as sequence boundaries, two are especially distinctive. These are the base of the postglacial cap carbonate at the top of the Blaini Formation, and the regional flooding surface at or close to the Krol–Tal contact (surfaces 1 and 8 in Figs. 2–4).

SEQUENCE BOUNDARIES

Surface 2

Surface 2 is located at or near the contact between the Infra Krol Formation and the Krol Sandstone (Figs. 3, 4). It is best expressed in the Solan area (V.K. Srivastava, personal communication 1994) and at Nainital syncline (sections G and A in Figs. 3 and 4), two locations at which shale, siltstone and thin-bedded very fine-grained sandstone are overlain abruptly by 30 to 60 m of coarser-grained sandstone (Fig. 10). In the Nigalidhar, Mussoorie, and Garhwal synclines (sections F to B in Figs. 3 and 4), the surface is cryptic, and is thought to be expressed in each case by the top of a sanding-upward interval up to several tens of meters thick (Fig. 10).

In the Solan area, the sandstone unit is mapped as the Krol Sandstone. It is composed of three to four fining-upward units, each consisting of pebbly sandstone and coarse- to medium-grained sandstone, passing upward into medium- to fine-grained sandstone and siltstone. Although it is not possible to trace the lower boundary of the sandstone continuously in available outcrop, the abrupt grain-size change at the base, the internal facies architecture, and marked changes in thickness between adjacent sections over a distance of several kilometers suggest the presence of an erosional unconformity with more than 50 m of relief. The sandstone is composed of well-rounded and well-sorted quartz grains, and it contains abundant trough and tabular cross-stratification, and small-scale ripple cross-lamination (Fig. 10). It has been variously interpreted as eolian (Auden 1934), shallow marine (Bhattacharyya and Chanda 1971), neritic–littoral (Bhattacharya and Niyogi 1971), and intertidal to subtidal sand bars (Bhargava and Singh 1981). On the basis of facies architecture, we tentatively interpret the sandstone as fluvial to estuarine (cf. Van Wagoner et al. 1990; Levy et al. 1994; Zaitlin et al. 1994; Christie-Blick 1997; Rossetti 1998). A sandstone unit observed at the same stratigraphic level in the Nainital syncline is

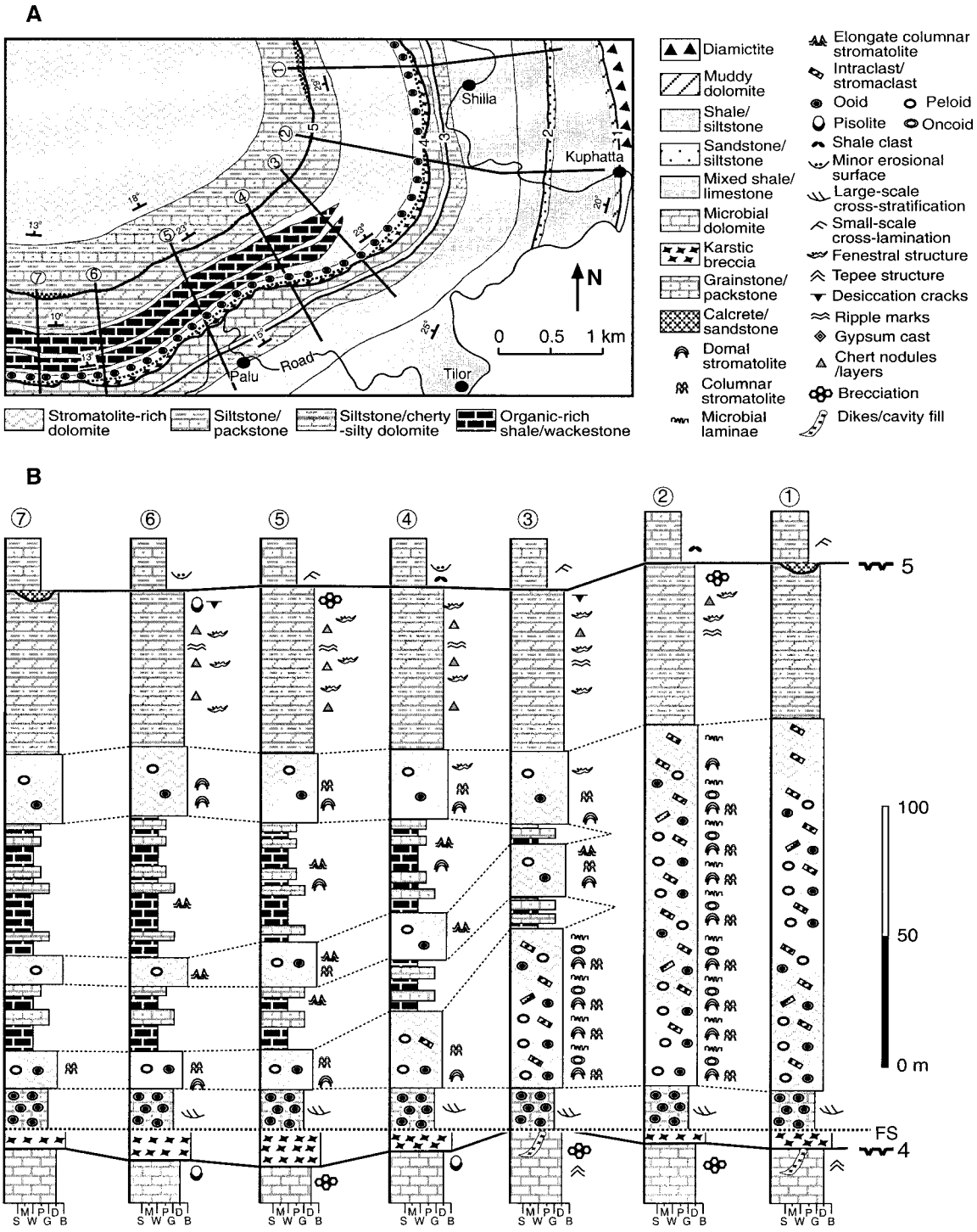

FIG. 5.—**A)** Map of a portion of Nigalidhar syncline showing the main facies, location of surfaces 1 to 5, and measured sections. Note interfingering relationship between stromatolite-rich dolomite and organic-rich shale–wackestone. **B)** Segments of selected measured sections showing vertical and lateral facies relationships, and evidence for karst development at sequence boundaries 4 and 5.

very similar to the Krol Sandstone but is documented at only one section. If the thickness of the sandstone is a measure of erosional relief, that may exceed 60 m in the Nainital syncline (Fig. 10).

The top of the sandstone is marked by a distinctive, 20- to 50-cm-thick, muddy–silty dolomite, which is overlain in turn by green to black shale lacking obvious sedimentary structures. This lithic discontinuity is present in all synclines, even where the sandstone unit is absent (Fig. 10). In the Solan area and in the Nainital syncline, a 5- to 15-cm-thick lenticular pebble conglomerate immediately below the dolomite layer is composed mainly of fragments from the underlying stratigraphy, and is interpreted as a lag at a flooding surface. The absence of evidence for subaerial exposure or erosion at this level in the Nigalidhar, Mussoorie, and Garhwal synclines is ascribed to a combination of less favorable outcrop and incomplete mapping of the Infra Krol Formation; a paleogeographic location removed from rivers, where valley incision would have been localized (cf. Woolfe et al. 1998; Talling 1998);

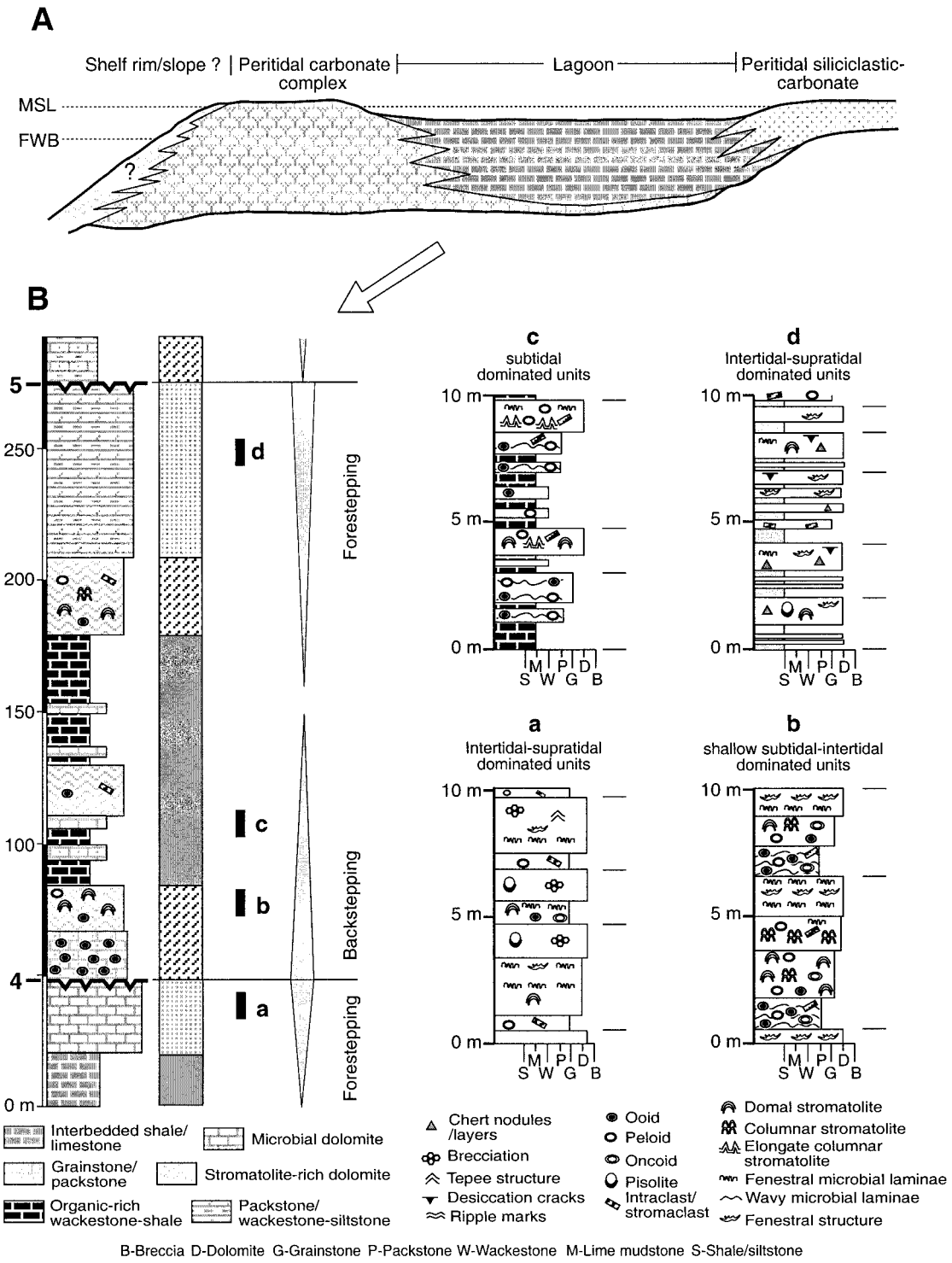

FIG. 6.—**A)** Lateral facies distribution in middle part of Krol Group from northwest (left) to southeast (right). **B)** Example showing facies stacking patterns between surfaces 4 and 5. The section is from the Nigalidhar syncline (section 4 in Figure 5). Note that small-scale shallowing-upward units do not necessarily represent equal spans of time.

and modification of the sequence boundary during marine flooding. The presence of sandstone-filled valleys at opposite ends of the Lesser Himalaya does not necessarily have any particular significance. The paleogeography is inherently more complicated than might be implied by a single oblique cross section (Figs. 3, 4), and it undoubtedly changed during deposition of the Infra Krol Formation and Krol Group.

Surface 4

Surface 4 is located in the lower part of Krol C and is the most prominent and well-defined surface in each syncline. It is regionally mappable, with up to 50 m of local relief, and in many places it is overlain by breccia of inferred paleokarstic

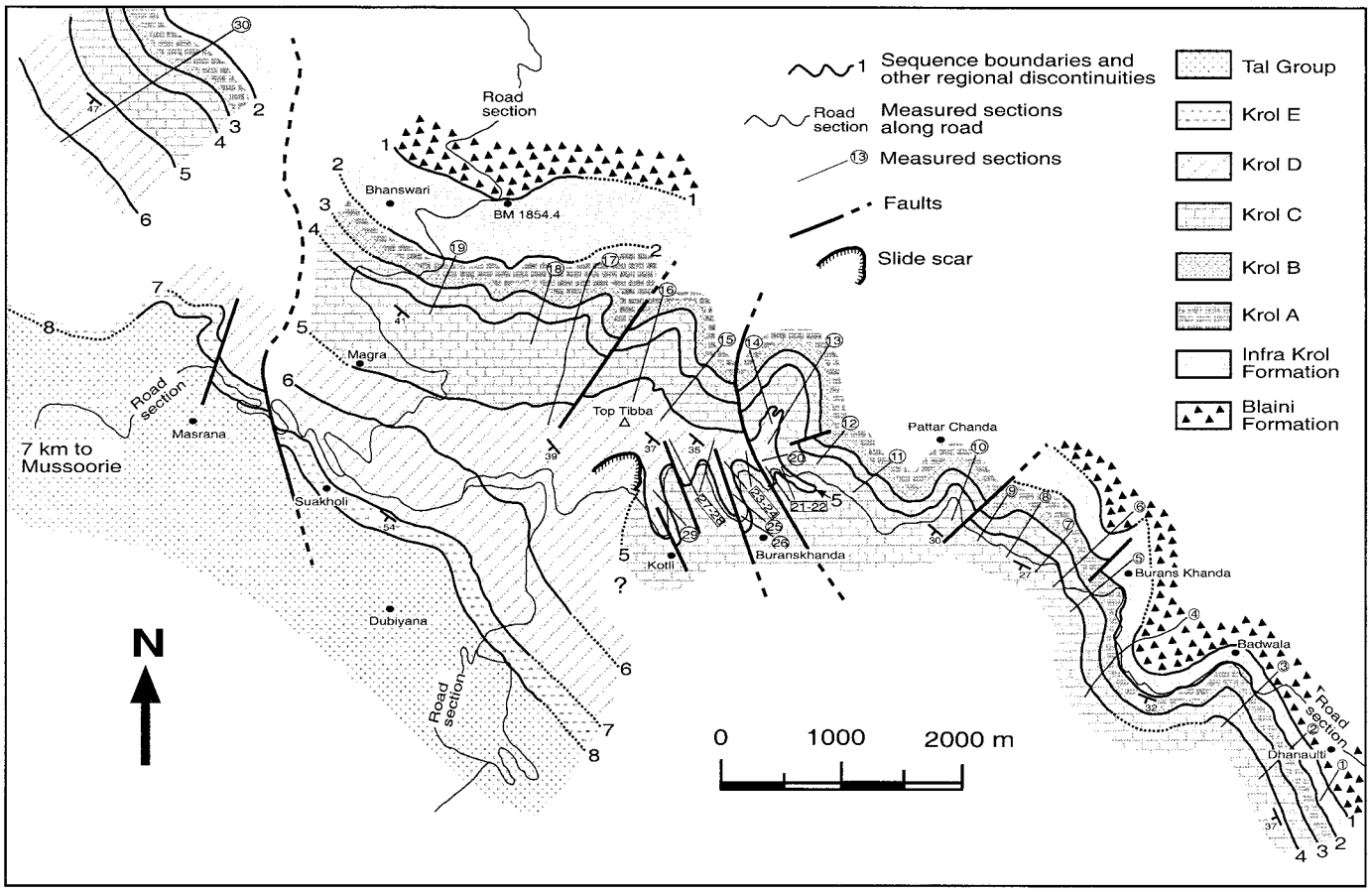

FIG. 7.—Map of a portion of the north limb of the Mussoorie syncline, showing lithostratigraphic units, sequence boundaries and other regional stratigraphic discontinuities, and measured sections.

origin. Both mantling and collapse breccias are present, along with vertical sediment-filled and cement-filled fissures, and smaller-scale solution-related features. At Nainital syncline, breccia is overlain by up to 40 m of lenticular sandstone (section A in Fig. 3) interpreted as an incised-valley fill or a karst-valley fill. The facies stacking pattern changes abruptly at the surface from upward shoaling to upward deepening, an observation that both supports the sequence boundary interpretation and provides a criterion for mapping the surface where breccia is absent.

Karstic Landforms.—Karstic landforms are well expressed at surface 4 in all five synclines by depressions of various sizes and shapes, and by intra-depressional stratigraphic highs (cf. Jennings 1985; Choquette and James 1988; Pelechaty et al. 1991). In the best developed examples, in the Mussoorie and Nainital synclines (Figs. 11, 12), up to 30 to 50 m of local relief is documented by correlation of key beds between closely spaced sections and by mapping along extensive cliff exposures. Depressions vary from symmetrical to asymmetrical in cross section, in some cases containing sub-depressions within a larger feature (Fig. 11). Overlying both karstic breccias and adjacent highs is 20 to 30 m of transgressive ooid grainstone–packstone. These rocks are overlain in turn by interbedded organic-rich shale and wackestone, which are interpreted to represent the deepest-water facies of the overlying sequence (Figs. 11, 13A). In the Nainital syncline, the most prominent depression is only partially filled by karstic breccia. This is overlain by up to 40 m of greenish-gray medium- to coarse-grained sandstone and siltstone, also localized within the depression (Fig. 12). The first unit to extend beyond the limits of the karstic depression is composed of shale and wackestone that, as in the Mussoorie syncline, represents a relatively deep lagoonal environment. More modest depressions have been observed at the same stratigraphic level in the Mussoorie and Nigalidhar synclines, and at Solan (Fig. 13). These are commonly associated with nearly vertical or step-like walls in cross section, and they are interpreted as sinkholes (or dolines) and karstic valleys, depending on their three-dimensional geometry. Similar morphologic features have been documented in numerous examples of modern and ancient karst (e.g., Jennings 1985; Kerans and Donaldson 1988; Pelechaty et al. 1991).

In the vicinity of stratigraphic highs between depressions, surface 4 is commonly planar and approximately parallel to stratification in both underlying and overlying rocks. Lenses of intensely silicified or dolomitized breccia are present locally, along with smaller-scale solution features such as fissures and vugs. Ooid grainstone found within fissures shows that these features were open during transgression. Where only vugs are present, the surface is commonly subtle, and lateral tracing is needed to verify the spatial connection with more obvious karstic features. Stratigraphic highs vary in width from hundreds of meters within composite depressions to several kilometers. Broad highs are interpreted as karst plains; narrow highs are interpreted as karst towers (Maslyn 1977; Jennings 1985; Choquette and James 1988).

Breccias.—Breccias associated with these karstic features are of two kinds, polymict and monomict, although there is commonly no sharp contact between them where they are present together. Polymict breccias (Fig. 13C) in many cases overlie the karstic unconformity as irregular sheets or smaller patches in topographic lows. They are typically composed of a mixture of sharp-edged carbonate fragments and chert rubble, together with less common blocks of pedogenic pisolite (paleosol), claystone, and green shale. Interstices between blocks are filled by siltstone, sandy dolomite, or dolomitic sandstone, each of these rock types in places strongly silicified. Monomict breccias are characterized by relatively homogeneous clast composition, consistent with that of associated *in situ* stratigraphy. Interstices in these breccias are filled by sandy dolomite, siltstone, or claystone. Polymict breccias are interpreted as mantling breccias (Choquette and James 1988; Kerans and Donaldson 1988). Monomict breccias are thought to be related to the collapse of cave ceiling (Choquette and James 1988; Kahle 1988). Interstratification of these breccias at Mussoorie syncline (Fig. 11) may be due to multiple stages of collapse, with mantling breccias being transported through a cave or karst valley system between episodes of collapse.

The breccias are thought to be paleokarstic, and not related modern karst. They are stratigraphically restricted and laterally persistent. They fill fissures and are overlain with sharp contact by younger stratigraphic units. Solution features such as pipes, which might connect the breccias with younger or modern karst, are absent in the immediately overlying beds (cf. Wright 1982). Breccia fragments are reworked into overlying ooid grainstone–packstone and, at Nainital, into sandstone.

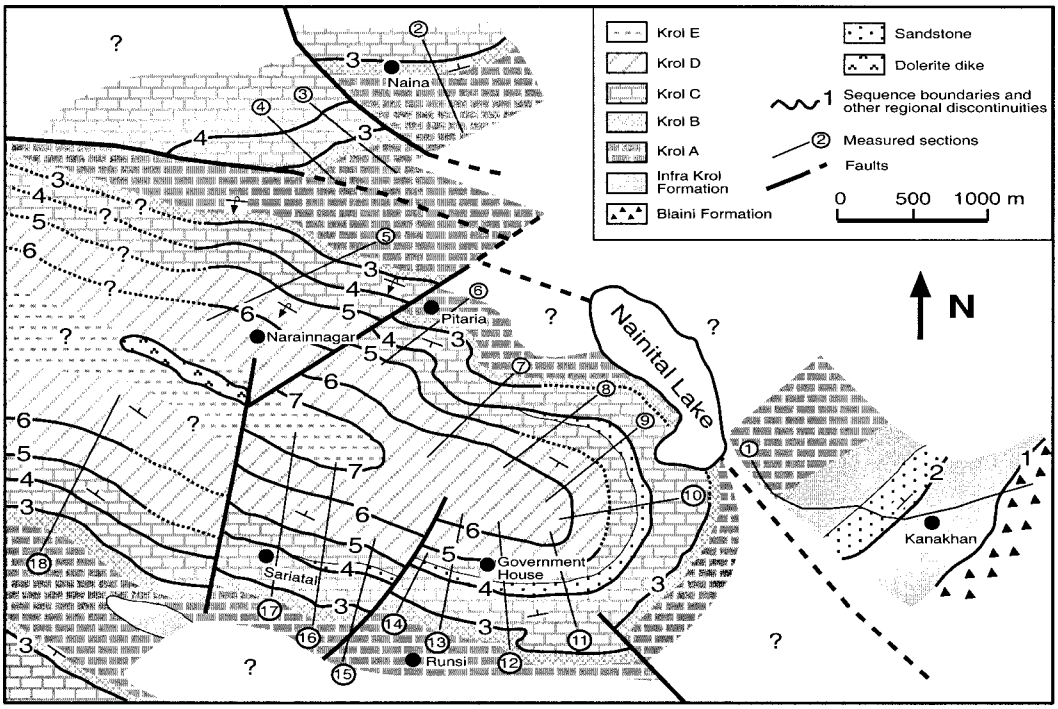

FIG. 8.—Map of a portion of the Nainital syncline, showing lithostratigraphic units, sequence boundaries and other regional stratigraphic discontinuities, and measured sections (remapped after Misra 1992).

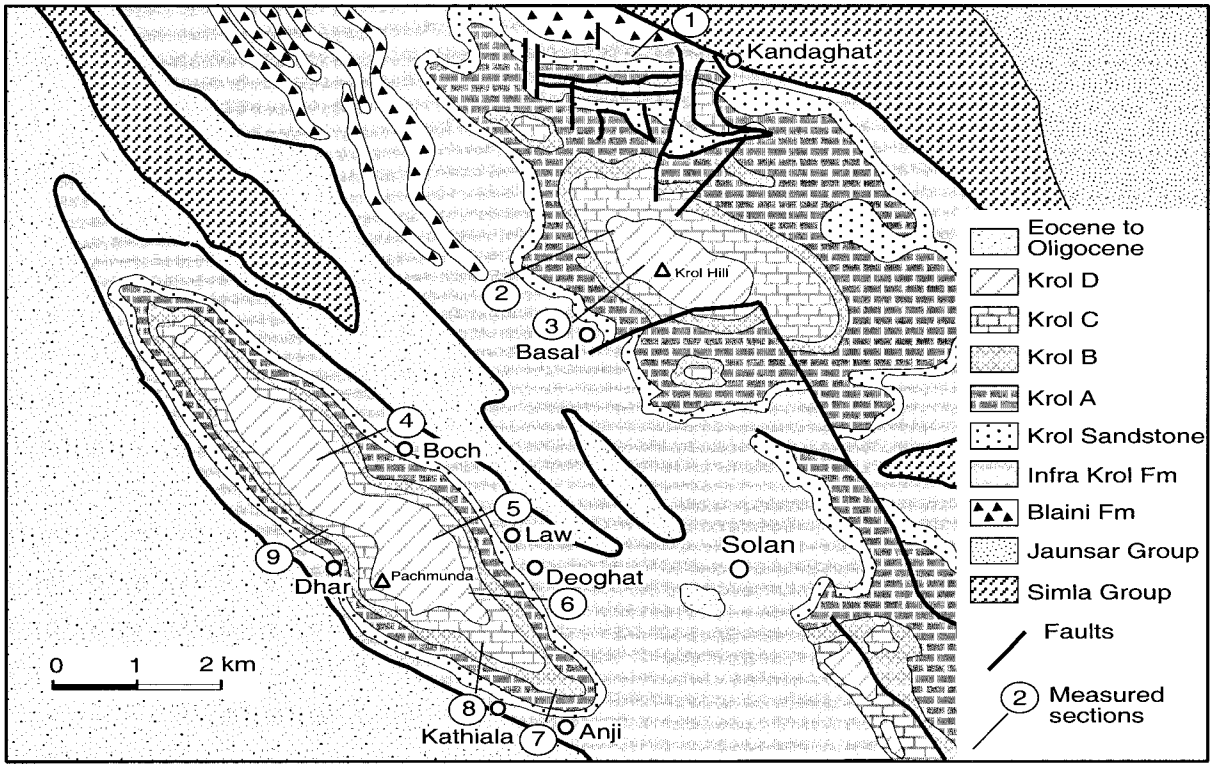

FIG. 9.—Geological map of Solan area (modified from Bhattacharya and Niyogi 1971), with location of measured sections.

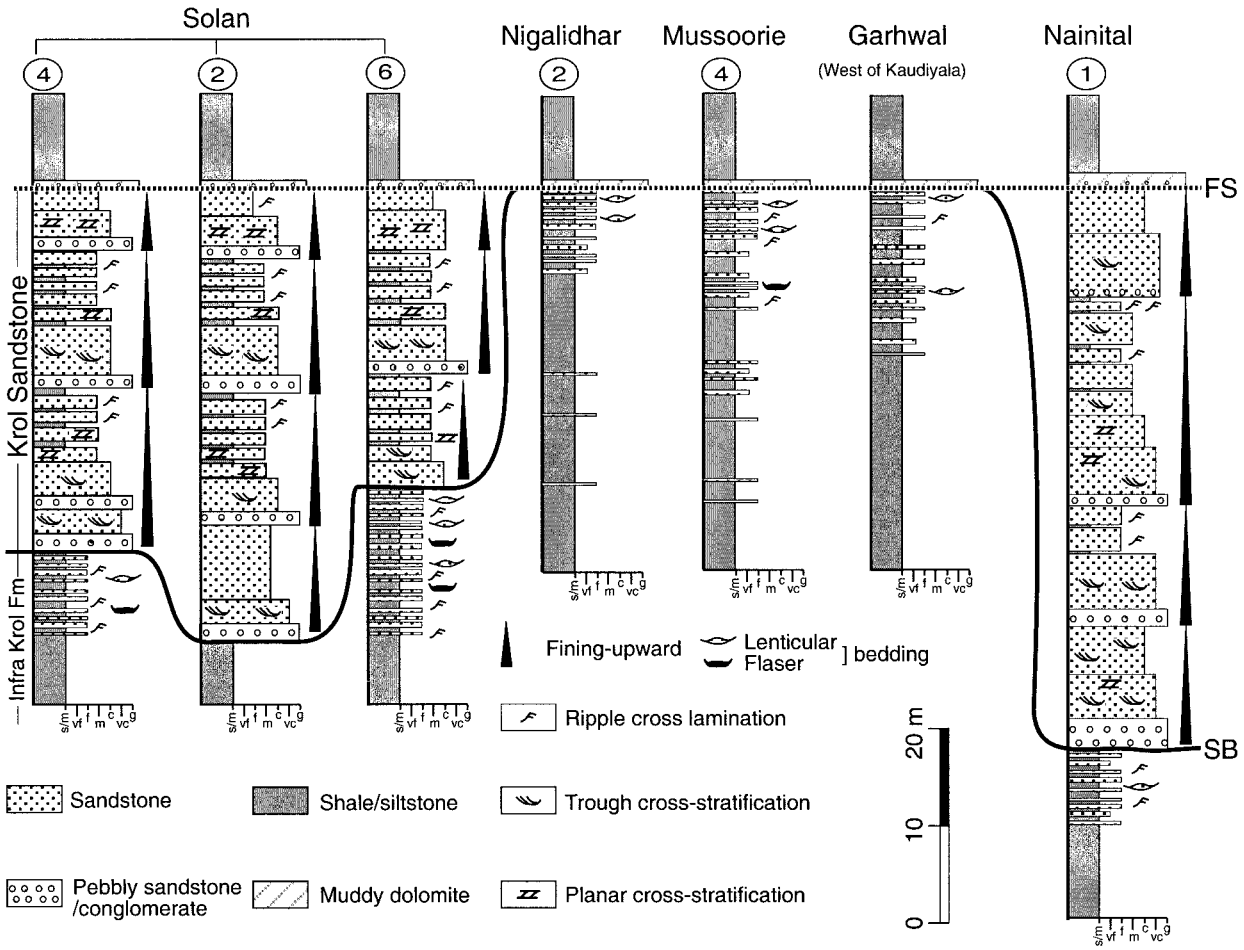

FIG. 10.—Representative measured sections across sequence boundary 2 (SB). For location of sections, see Figures 5A (Nigalidhar syncline), 7 (Mussoorie syncline), 8 (Nainital syncline) and 9 (Solan area). Section at the Garhwal syncline is ~ 5 km west of Kaudiyala village flooding surface. Column width is calibrated to Wentworth grain-size scale.

Sandstone.—The lenticular sandstone that overlies karstic breccia at Nainital syncline (Fig.12) is composed of an upward-fining succession of greenish-gray to grayish-red medium- to fine-grained quartz sandstone and siltstone, with dispersed carbonate clasts near the base (Fig. 12). Trough and tabular cross-stratification and ripple cross-lamination are present but not common. In the cliff east of Sariatal (section 16 in Fig. 8), interbedded siltstone and sandstone is found to onlap karstic breccia at an angle of 10° to 15°.

The sandstone unit is interpreted as a karst-valley or incised-valley fill owing to the presence of karstic breccia at the deepest level. The absence of sandstone or conglomerate as coarse as that observed at surface 2, along with both textural and compositional maturity, suggest that the sandstone may have accumulated at least in part during subsequent transgression. It is unclear whether or to what extent fluvial processes were involved in the development of this unit.

Solution-Related Surface and Subsurface Features.—Smaller-scale solution-related features are widely distributed along depressions and stratigraphic highs. These include downward-projecting fissures, cavities filled with siltstone or dolomitic fine-grained sandstone (Fig. 13D), smaller voids, and concave-upward curved surfaces, which may represent scallops or karren (Choquette and James 1988; Desrochers and James 1988). These features are exposed only in the cross section and have not been observed in the plan view. They are interpreted as paleokarst-related features because they are closely associated with the unconformity surface, and increase in abundance upwards towards that surface.

Change in Facies Stacking Pattern.—The overall succession from surface 3 to surface 4 displays a shoaling-upward trend: from shallow subtidal dominated units to intertidal–supratidal dominated units, with the abundance of fenestrae, pedogenic pisolites, and vugs increasing upwards (Fig. 4). Above surface 4, the pattern changes abruptly to upward-deepening (Fig. 6B).

Surface 5

Surface 5 is located at or near the base of Krol D. Below the surface, vuggy, cherty dolomite with minor siltstone layers is interpreted as predominantly supratidal. Above it, interbedded siltstone–shale and dolowackestone–packstone (subtidal) are observed at Solan and at Nigalidhar, and Mussoorie synclines; and cherty dolomite and siltstone (intertidal) at Garhwal and Nainital synclines (Figs. 3, 4, and 14). In contrast to the well developed karst features observed at surface 4, this surface is much more subtle, but it nevertheless exhibits evidence for subaerial exposure in the form of small-scale depressions and dissolution cavities filled with karstic breccias, siltstone, calcrete lenses, and sandstone; relict paleosols; and pebbly sandstone lags. As at surface 4, there is a marked change in facies stacking, from upward shoaling to upward deepening. Examples of stratigraphic relations across the surface in each syncline are shown in Figure 14.

Depressions.—Small-scale depressions, 0.2 to 2.5 m deep and 2 to 15 m wide, have been observed at more than ten localities, including sections 2 and 3 near Solan (Fig. 9), sections 1 and 7 in the Nigalidhar syncline (Fig. 5), sections 17, 22, 24, 26, and 30 in the Mussoorie syncline (Fig. 7), and sections 13 and 15 in the mostly inaccessible cliffs of the Nainital syncline (Fig. 8). The depressions have steep walls and flat to bowl-shaped floors, and they are filled by a combination of breccia and sandstone–siltstone, with lenses of dolomudstone–lime mudstone that are interpreted as remnants of calcrete (see below; Fig. 15). The depressions are interpreted as closed, near-surface sinkholes or dolines in the exposed carbonate platform that were modified and filled during subsequent marine transgression (cf. Cvijic 1981; Jennings 1985; Vanstone 1998).

Paleosol Remnants.—Paleosol remnants have been observed widely along surface 5. They are expressed as discontinuous layers of grayish-red, yellow and buff-colored massive siltstone and fine- to very fine-grained sandstone, with dolomud-

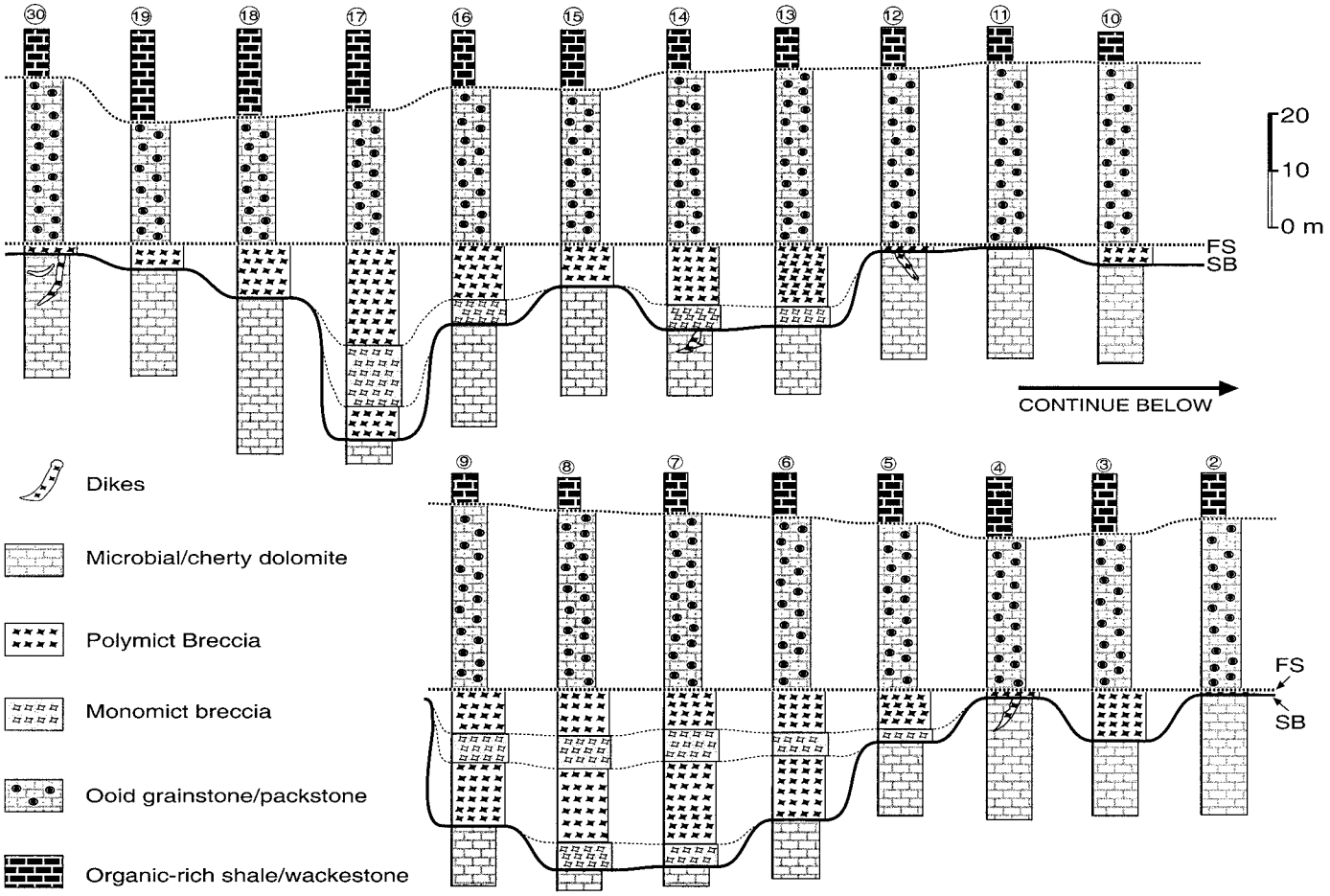

FIG. 11.—Measured sections across sequence boundary 4 (SB) at the Mussoorie syncline, showing karstic depressions filled with polymict and monomict breccias. See Figure 7 for location of sections. FS, flooding surface.

stone–lime mudstone nodules or lenses and pedogenic pisolites, nodules of chert and iron oxide, and breccia (Fig. 14; cf. Mustard and Donaldson 1990; Pelechaty and James 1991; Vanstone 1991; Wright 1994; Joeckel 1999). These rocks fill small depressions and rest on brecciated cherty dolomite (Fig. 14).

Lag Deposits.—Pebbly sandstone lags are found locally along the surface. They consist of cherty dolomite clasts in a fine-grained sandstone matrix, in which quartz particles are well rounded and well sorted. Lithoclasts are 1 to 5 cm across, angular to subrounded, and poorly sorted. Most of the clasts are compositionally identical to underlying beds. Siltstone clasts 2 to 7 mm across are found in siltstone beds directly overlying the unconformity at Nigalidhar and Mussoorie synclines (Fig. 14). These lags and siltstone clasts are interpreted to represent a regolith that developed on the unconformity and that was reworked but not completely removed by waves and currents during subsequent marine transgression.

Other Solution-Related Subsurface Features.—Vugs and small solution cavities are found below the surface, but obvious surface karstic features (e.g., karrens) and large grikes have not been observed. Vugs are widely distributed for several tens of meters below surface 5, but larger cavities, several centimeters to several meters across, are restricted to the uppermost 10 m. These range from bowl-like to flask-shaped, and they are filled with dolomudstone or lime mudstone.

Change in Facies Stacking Pattern.—With the exception of the Solan area, the interval between surfaces 4 and 5 is characterized by upward deepening from shallow subtidal–intertidal dominated units to subtidal dominated units (backstepping), and then upward shoaling again to intertidal–supratidal dominated units (forestepping, Fig. 6B), with fenestrae, pedogenic pisolites, vugs, tepees, desiccation cracks, and brecciation increasing in abundance towards surface 5 (Fig. 3). As at surface 4, this trend changes abruptly at the contact with the onset of transgression.

OTHER REGIONAL STRATIGRAPHIC DISCONTINUITIES

In addition to the three surfaces described above, five additional regional discontinuities have been identified on the basis of a change in facies stacking pattern, abrupt facies changes in individual sections, and regional persistence from one syncline to another, but with little or no evidence for karstification or erosion (Figs. 3, 4). They are interpreted as regional flooding surfaces.

Surface 1

Surface 1 is the sharp contact near the top of the Blaini Formation between glacial–marine diamictite and the cap carbonate. The cap carbonate is typically 5 to 15 m thick, and is composed chiefly of silty laminated dolomite, in places interstratified with very thin beds of shale. The absence of wave- or current-agitated structures suggests deposition in relatively deep water, as is typical of cap carbonates (Kennedy 1996). Overlying rocks consist of as much as several hundred meters of green to black shale, siltstone, and minor fine- to very fine-grained quartz sandstone. Sedimentary structures are rare, mostly parallel lamination and small-scale ripple cross-lamination. The paleo–water depth is inferred to have been relatively deep (below storm wave base), although an upward increase in the abundance of cross-laminated sandstone suggests shoaling towards surface 2.

Surface 3

Surface 3 is located at or near the Krol B–Krol C contact. Underlying strata are interpreted to shoal upwards from shale and lime mudstone (deep subtidal) to shale–siltstone and ooid wackestone–packstone (shallow subtidal; Krol A), to grayish-red siltstone and silty dolomite with desiccation cracks and gypsum casts (intertidal–supratidal; Krol B; Figs. 3, 4). Immediately above the surface, shallow-water indicators disappear abruptly. Basal beds of Krol C consist of unevenly interbedded green to black shale, lime mudstone, and dolowackestone (shallow subtidal). No evidence for subaerial erosion has been observed at any of the localities studied.

Surface 6

Surface 6 is located in the upper part of Krol D. It is expressed by a transition in facies stacking pattern from forestepping to backstepping at Solan, and in the

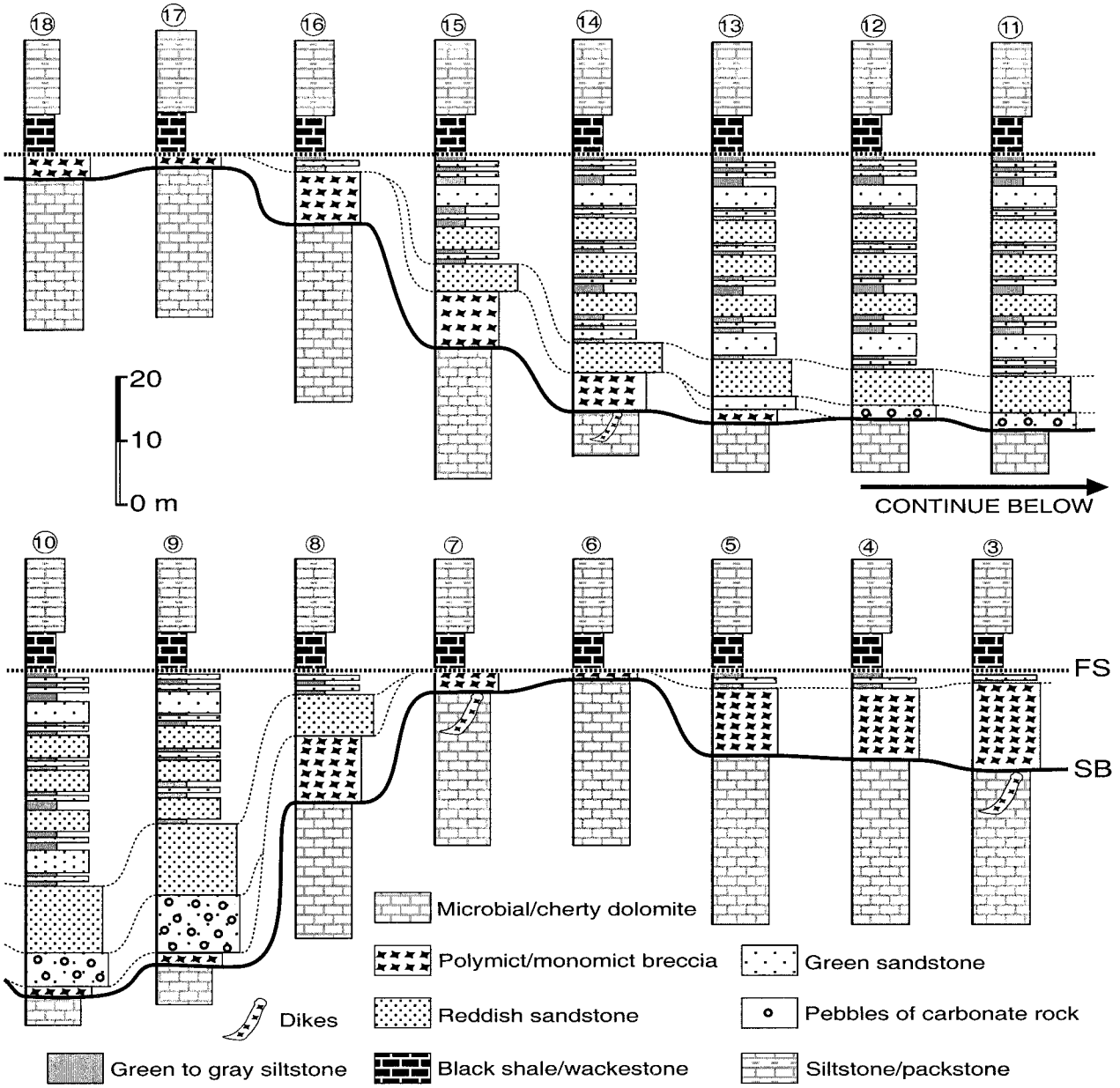

FIG. 12.—Measured sections across sequence boundary 4 (SB) at the Nainital syncline, showing karstic depressions filled with breccias, sandstone and siltstone. FS, flooding surface. See Figure 8 for location of sections.

Nigalidhar and Mussoorie synclines, and by an abrupt facies change across the surface in the Garhwal and Nainital synclines. At Solan and in the Nigalidhar syncline, the succession between surfaces 5 and 6 is characterized by an overall forestepping pattern from subtidal dominated units to peritidal dominated carbonate units, with shallow-water features such as fenestrae, tepee structures, pedogenic pisolites, and brecciation increasing in abundance upwards toward surface 6. In the Mussoorie, Garhwal, and Nainital synclines, the succession is characterized initially by backstepping, followed by forestepping with an increase in the terrigenous component and shallow-water features, including fenestrae, tepees, and desiccation cracks. Surface 6 is overlain abruptly by dolowackestone–packstone and shale (shallow to deep subtidal). Lateral pinch-out of the former at Garhwal and Nainital synclines may be due to subtle regional onlap.

Surface 7

Surface 7 is located at or near the Krol D–Krol E contact, and it has been studied only in the Mussoorie, Garhwal, and Nainital synclines. In the Mussoorie and Garhwal synclines, the section below the surface is composed of up to 130 m of massive cherty dolomite with peritidal features, such as fenestrae, tepees, pedogenic pisolites, and local brecciation. This unit is overlain at the surface by interstratified siltstone and silty dolomite, and those are overlain in turn with a deepening-upward trend by greenish-gray shale. In the Nainital syncline, immediately below the surface, interbedded siltstone and cherty silty dolomite with minor fine-grained sandstone contains desiccation cracks. This unit is overlain abruptly by thick shale in which no water-depth trend can be discerned. Although facies below the surface vary from one syncline to another, evidence for subaerial exposure, especially pedogenic pisolites, abundant fenestrae, and tepees, disappear abruptly at this level. As at surface 6, the pinch-out of carbonate rocks above the surface may be due to regional onlap (Fig. 3). In the Garhwal syncline, small-scale dissolution cavities are found below the surface, and small-scale scours filled with fine-grained sandstone have also been seen. In the Mussoorie syncline, geopetal rings (isopachous cement growing downwards and coating pisolites) are observed below the surface. Surface 7 is a candidate for a sequence boundary, but better outcrops are needed to establish definitive evidence.

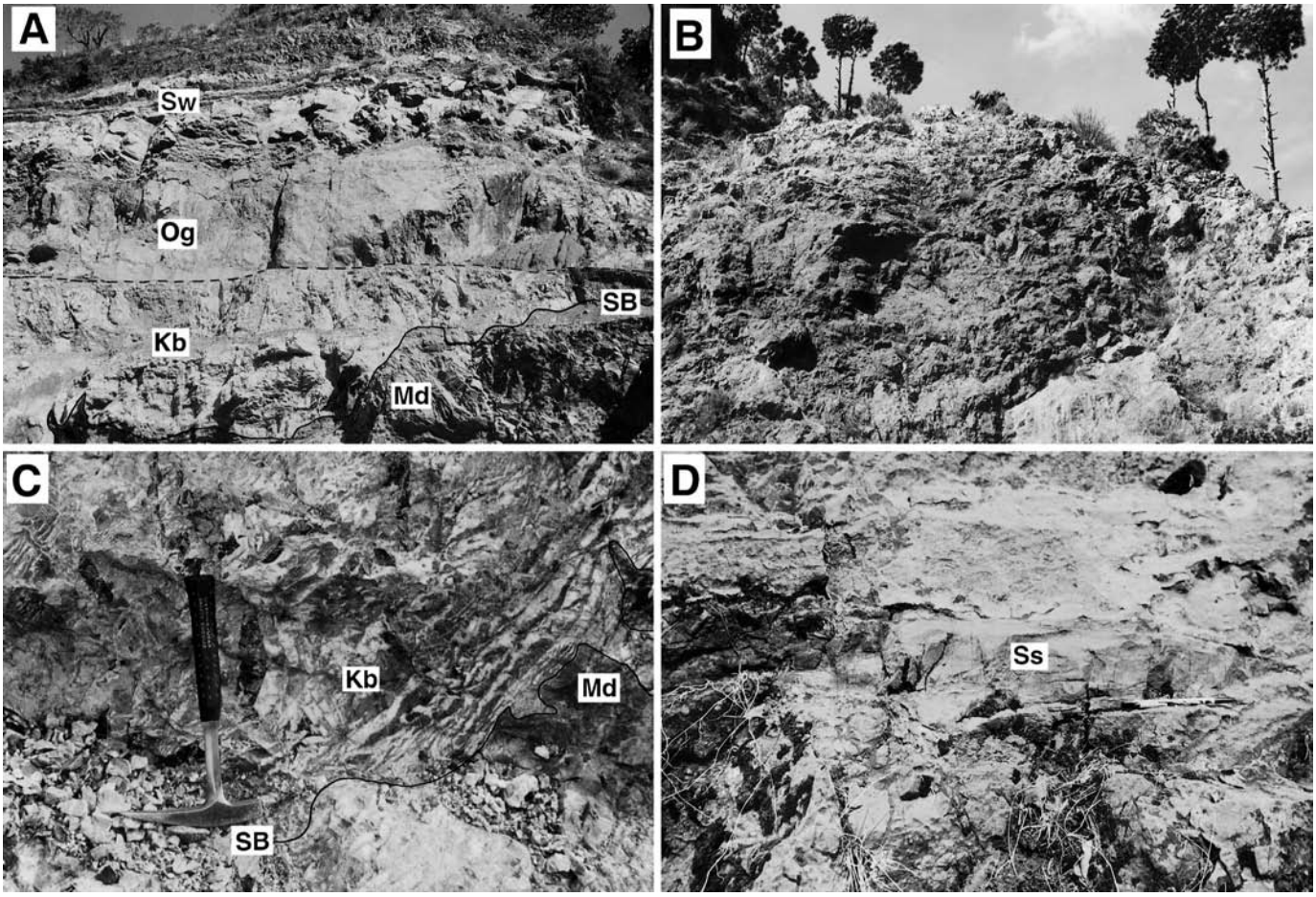

FIG. 13.—Karstic features at sequence boundary 4 (SB). **A)** Dolomitized karstic breccia (Kb) filling karstic depression above microbial dolomites (Md), and overlain by ooid packstone–wackestone (Og), and black shale and wackestone (Sw). Outcrop located near Dubra on southern limb of the Mussoorie syncline. Thickness of section shown is ~ 42 m. **B)** Bowl-shaped depression with breccia fill exposed in Solan area (near section 5 in Fig. 9). **C)** Silicified polymict breccia (Kb) overlying microbial dolomites (Md), Nigalhidar syncline (near section 7 in Fig. 5). Note upward increase in degree of brecciation. **D)** Solution cavity filled with dolomitic fine-grained sandstone (Ss), Nainital syncline (near section 3 in Fig. 8). Cavity is oriented parallel to bedding and is 10 m below breccia at unconformity.

Surface 8

Surface 8 at or near the Krol–Tal contact (Precambrian–Cambrian boundary) has been studied in limited outcrops in the Nigalidhar, Mussoorie, and Garhwal synclines. It is marked by a regionally persistent, abrupt facies change between muddy dolomite of Krol E and highly condensed black shale, chert, and phosphorite of the basal Tal Group. Below the surface, muddy dolomites of the uppermost Krol E unit contain fenestrae, microbial laminae, and lenses of gypsum, features that are characteristic of intertidal environments. At Mussoorie syncline, a 2- to 5-cm-thick lenticular ferruginous claystone may represent a relict paleosol. The basal Tal Group lacks shallow-water indicators, and it is interpreted as a relatively deep-marine facies assemblage. Pyrite, which is abundant in the shale and phosphorite in the form of syngenetic to diagenetic layers (Banerjee et al. 1997), suggests an anoxic depositional setting.

DISCUSSION

Development of Karstic Surfaces

Numerous studies of modern and ancient karst features suggest that the most favorable conditions for prominent karstification include the following: (1) marked base-level lowering (e.g., Choquette and James 1988; Beach 1995; Tinker et al. 1995; Lucia 1995); (2) moderate to high rainfall (e.g., Budd et al. 1993; Mylroie and Carew 1995; Wagner et al. 1995; Palmer 1995); and (3) relatively pure, dense, and thick carbonate rocks with appropriate conduits such as fractures, joints, faults, or selective solutional pipes (e.g., James and Choquette 1984; Jennings 1985; Bosák et al. 1989; Palmer 1991; Cander 1995; Smith et al. 1999). Contrasting examples of karst development in the Krol platform reflect the interplay of these factors (Fig. 16).

Surface 4 developed under conditions favorable for prominent karstification, with tens of meters of base-level lowering superimposed upon a regionally persistent unit of microbial dolomite (Fig. 16A). Subaerial exposure, along with the presence of appropriate fractures, created the aquifer system needed for the development of large caves or dolines (stage 2 in Fig. 16A). Polymict breccias derived from the Earth's surface, monomict breccias related to the collapse of roofs and walls, and sandstone–siltstone derived from the proximal side of the platform gradually filled the caves and dolines prior to the onset of transgression (stages 3 and 4 in Fig. 16A). Independent information about the climate is not readily available. However, the absence of calcrete at surface 4 suggests relatively humid rather than arid conditions (Read 1995).

In contrast, surface 5 appears to have developed under conditions less favorable for penetrative karstification (Fig. 16B). The cherty dolomite and siltstone that characterizes many of the locations studied and the massive dolomites of the Solan area (Figs. 3, 4) would have inhibited the development of karstic landforms. The maximum relief along the surface may have been limited to the thickness of the uppermost carbonate layer whatever base-level change was involved. After transgression only relict paleosols and small depressions were left along the surface (stage 4 in Fig. 16B). The presence of abundant calcrete indicates an arid to semiarid climate (Read 1995).

For surface 7, pedogenic pisolites, fenestral structures, and brecciation are intense within the 50 m interval below the surface, but no depressions, dissolution cavities, or dikes have been observed along the surface. This may be due to modest base-level lowering and to the presence of carbonate sediments with pedogenic pisolites and cements that tended to resist meteoric dissolution (stages 2 and 3 in Fig. 16C). Subsequent drowning of the platform led to the development of a sharp lithological contact, but the surface itself is quite subtle (stage 4 in Fig. 16 C).

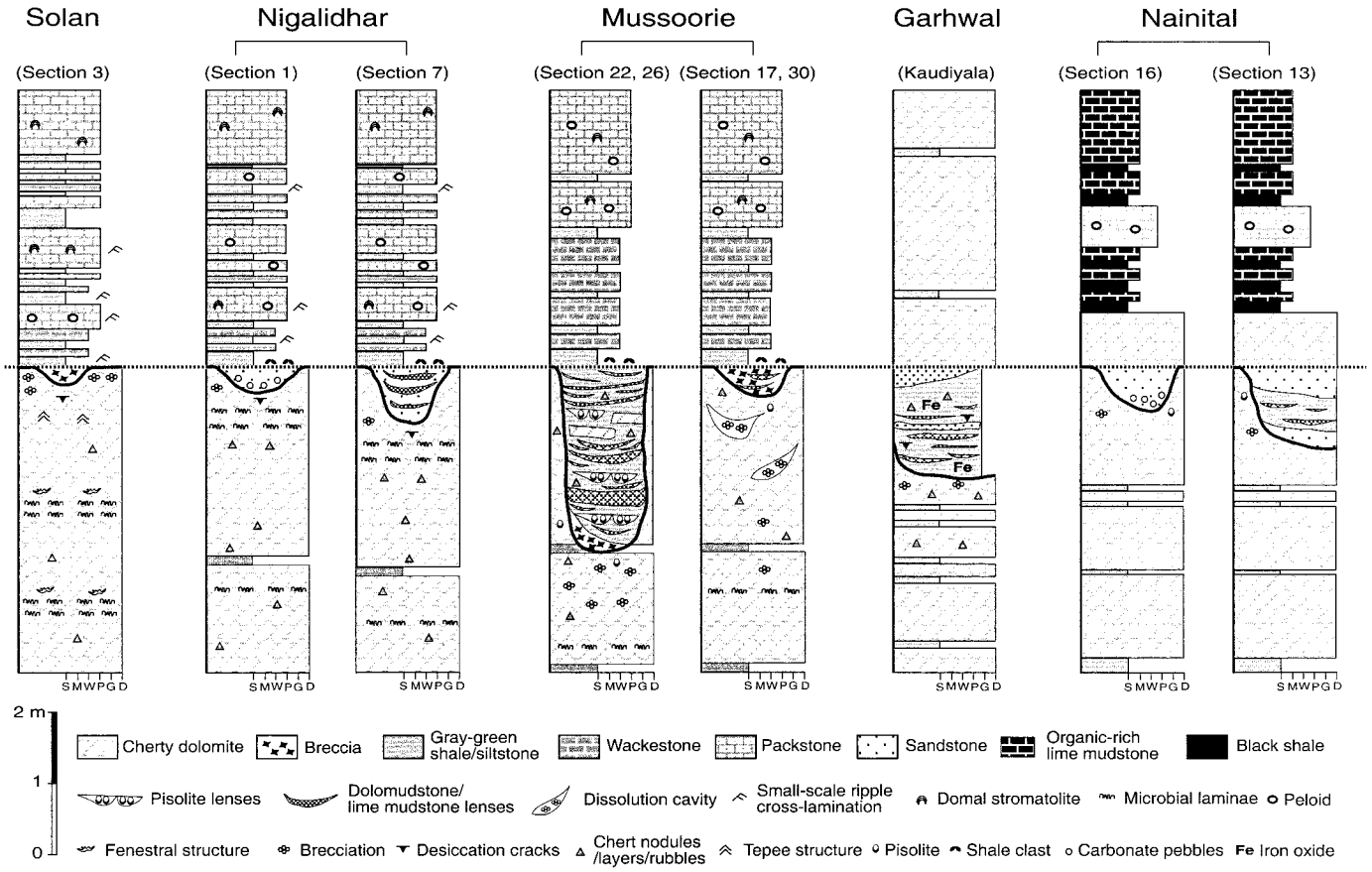

FIG. 14.—Selected sections across sequence boundary 5 (bold line), showing small depressions, depression fills and lag deposits. For location of sections, see Figures 5 (Nigalhidar syncline), 7 (Mussoorie syncline), 8 (Nainital syncline), and 9 (Solan area). Section at the Garhwal syncline is ~ 5 km west of Kaudiyala village.

Estimates of Base-Level Changes

The magnitude of base-level change associated with each sequence boundary can be estimated approximately from the erosional relief and character of early diagenesis observed at multiple locations along nearly 300 km of outcrop. The facies found below each surface accumulated in a peritidal environment. The scale of incised valleys documented at surfaces 2 and 4 suggests that base level was lowered by as much as 50 to 60 m (Figs. 10, 12). A comparable change in base level is permitted but not required at surface 5 (Fig. 16B). Base-level changes at other stratigraphic levels appear to have been modest.

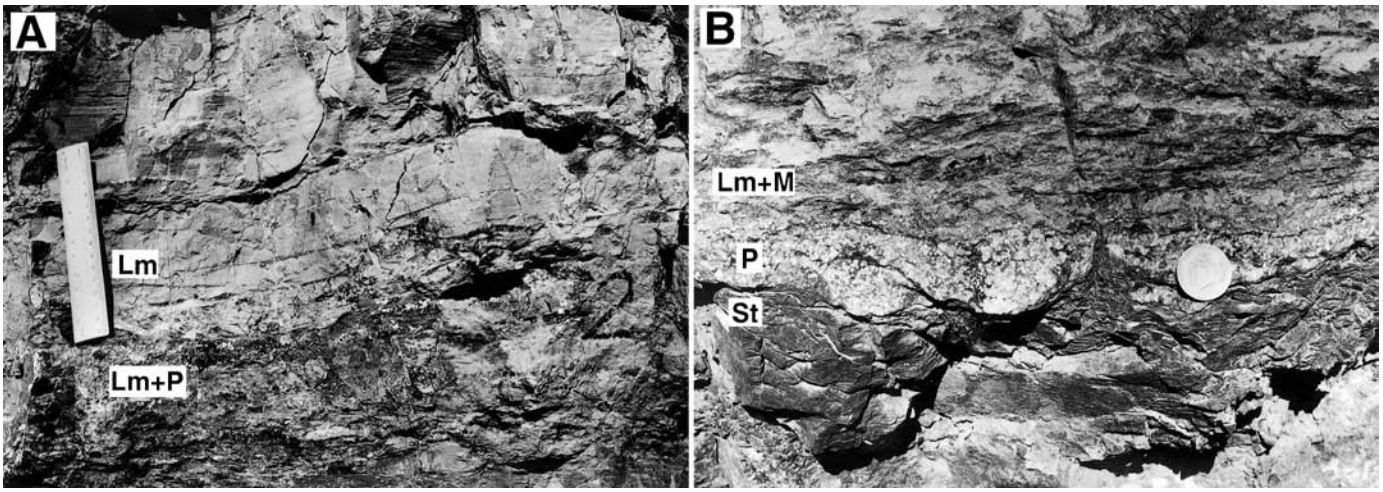

FIG. 15.—Selected features of calcretes at sequence boundary 5. **A)** Chertified lime mudstone and pisolites (Lm + P) overlain by massive and laminated lime mudstone (Lm), Mussoorie syncline, near section 26 in Fig. 7. **B)** Pedogenic pisolite lenses (P) overlying siltstone (St) and underlying lime mudstone and mudstone (Lm + M), immediately above surface 5, Mussoorie syncline, section 21 in Fig. 7.

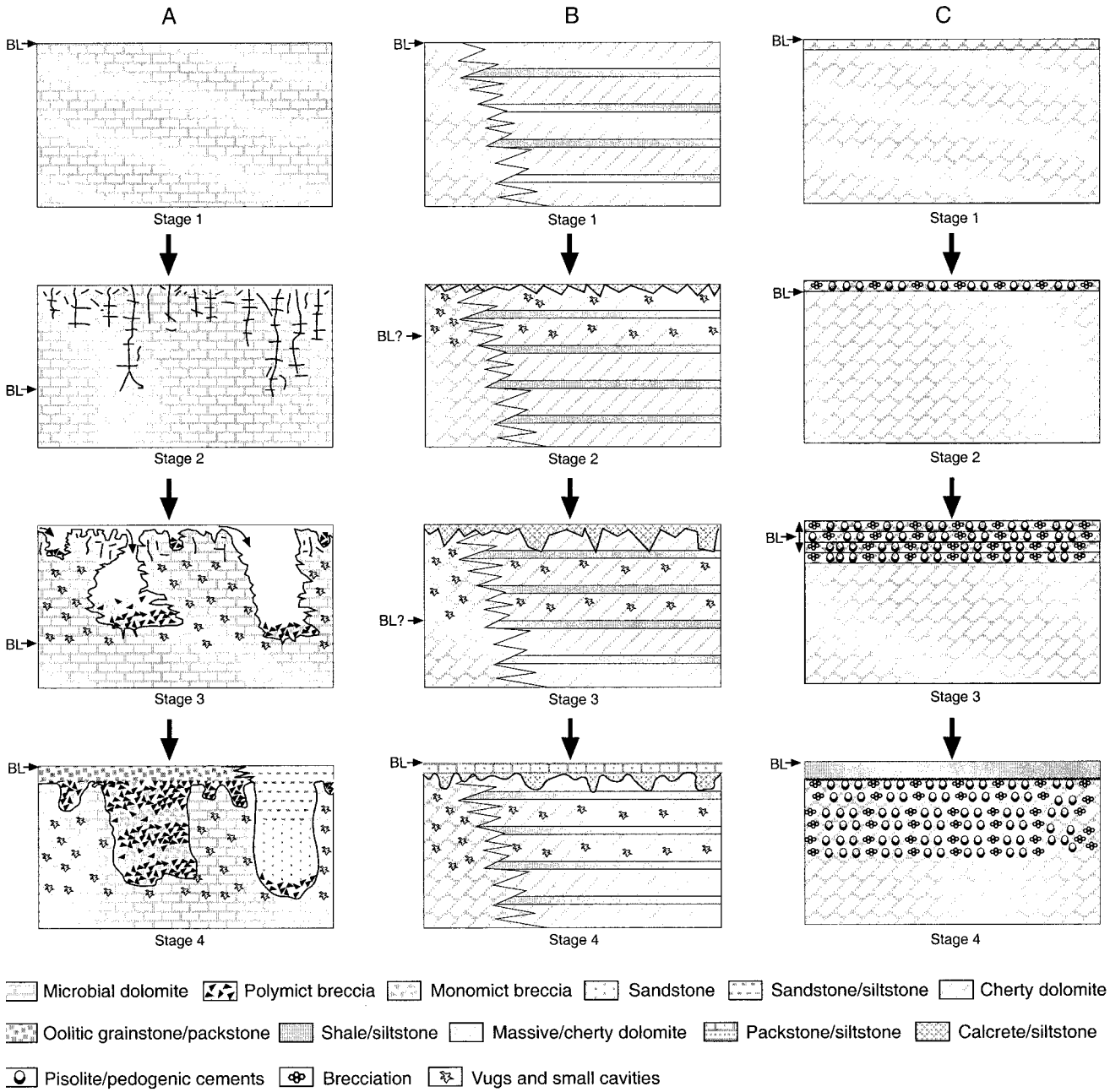

FIG. 16.—Schematic cross sections illustrating sequential development of features at surfaces 4, 5, and 7. **A)** Surface 4. Stage 1: Deposition of microbial dolomite before significant base-level lowering. Stage 2: Tectonic and/or eustatic lowering of base level (BL) leads to selective dissolution along fractures and development of aquifer system. Stage 3: Enlargement of fractures produces surface karst and caves (or dolines). Vugs and small-scale cavities develop in freshwater vadose and phreatic zones. Caves become partially filled with polymict breccias from topographic surface and monomict breccias from cave roofs/walls. Stage 4: Caves and dolines become closed and filled with breccia or sandstone–siltstone and buried by transgressive marine sediment. **B)** Surface 5. Stage 1: Deposition of the massive or cherty dolomite, interstratified with cherty dolomite and siltstone at shallow platform. Stage 2: Calcrete and karst develop only at topographic surface owing to resistance of available rock types to meteoric dissolution and absence of fractures. Vugs and small-scale cavities develop in the freshwater phreatic zone near water table. Stage 3: Karstification becomes intense at topographic surface but does not penetrate significantly into underlying layers owing to lack of connected aquifer system. Stage 4: Karstic surface is modified during transgression. Calcrete is preserved only locally along surface and in small depressions. **C)** Surface 7. Stage 1: Deposition of shallow marine carbonate layers in peritidal environment. Stage 2: Subaerial exposure results in induration and development of pedogenic pisolites, cements, and breccia. Stage 3: Small-scale fluctuations of base level result in cyclic deposition and exposure of carbonate sediments, with locally intense development of pedogenic pisolites and cements. Stage 4: Platform drowns during transgression. An abrupt facies transition is preserved but without obvious relief at the surface.

Constraints on the Timing of Neoproterozoic Glaciation

Recent studies have raised the possibility that there may have been as many as four ice ages during the later Neoproterozoic, at approximately 740, 720, 590 and 575 Ma (Kaufman et al. 1997; Saylor et al. 1998; Jacobsen and Kaufman 1999). Since no more than two glacial intervals are observed in most successions, the larger number has been doubted as an artifact of stratigraphic miscorrelation (Kennedy et al. 1998) or perhaps a function of the way in which glacial intervals are counted. Although Neoproterozoic glaciation was clearly extensive (Hoffman et al. 1998; Crowell 1999; Sohl et al. 1999), the interpretation of as many as four events implies

that during any given ice age, nonglacial facies would have accumulated over a significant portion of the planet. Existing correlation schemes hinge strongly on carbon and strontium isotope stratigraphy. Because postglacial cap carbonates are associated with pronounced negative carbon isotope excursions ($\delta^{13}C \sim -5‰$), carbon isotope minima (and negative excursions) have been interpreted as indicators of times of glaciation in nonglacial deposits (Kaufman et al. 1997; Jacobsen and Kaufman 1999). This hypothesis can be evaluated with reference to the Infra Krol–Krol succession of the Lesser Himalaya.

Widespread glaciation should have led to significant lowering of sea level, perhaps exceeding the ~ 135 m (~ 200 m water-depth equivalent) associated with Pleistocene glaciation (Fairbanks 1989), and at least as great as the several tens of meters of sea-level change associated with very modest Antarctic glaciation in the Oligocene (Kominz and Pekar 2001). Although it is difficult to quantify the amplitude of Neoproterozoic sea-level change, this expectation is supported by the existence of 160-m-deep valleys incised by rivers into braid-delta quartzite in the western U.S. at the level of the Marinoan glacial deposits of northwestern Canada (Christie-Blick 1997; Christie-Blick et al. 1999). Evidence has been documented in this paper for regional sequence boundaries at three levels in the Infra Krol Formation and Krol Group (surfaces 2, 4, and 5 in Fig. 2) and perhaps at one other stratigraphic discontinuity (surface 7). Although not required by available evidence, a eustatic (glacio-eustatic?) origin is permitted for each of the sequence boundaries, and given the scale of regional base-level change in what appears to be a passive-margin setting, this may be the most reasonable interpretation. Available evidence does not support significant base-level lowering at other stratigraphic levels. Nor is obvious evidence likely to have been missed in an intensive stratigraphic study over a distance of nearly 300 km.

Our carbon isotope data compiled from numerous sections are summarized in Figure 2, without making any judgment here about the significance of individual data points (details will be published elsewhere). The most striking feature of the data, beyond the degree of scatter at some stratigraphic levels, is that there is no correlation between isotopic minima and sequence boundaries, with the possible exception of surface 5. However, $\delta^{13}C$ values at that level range from $-6‰$ to $+9‰$, casting doubt on whether the negative isotopic values have any primary significance. The most prominent and persistent negative excursion, at the level of surface 3, is associated with no evidence in the rock record for the lowering of depositional base level, in spite of intense scrutiny with that expectation in mind. We infer that local diagenetic alteration or oceanographic phenomena unrelated to glaciation may be in part responsible for observed isotopic variation.

SUMMARY

Eight regional stratigraphic discontinuities have been identified in the postglacial Neoproterozoic succession of the Lesser Himalaya on the basis of (1) a transition in facies stacking patterns, typically from a forestepping to backstepping motif; (2) abrupt facies changes in individual sections; and (3) regional facies architecture. Three of the discontinuities (surface 2 in the Infra Krol Formation, and surfaces 4 and 5 in the Krol Group) are interpreted as sequence boundaries with one or more of the following lines of evidence for the lowering of depositional base level: (1) locally developed incised valleys; (2) large-scale paleokarstic depressions with mappable relief; (3) subaerial dissolution and weathering products (breccias and calcrete) filling vertical fissures, dikes, cavities, and shallow depressions in underlying carbonate rocks; and (4) small-scale evidence for subaerial exposure at an erosion surface.

Karst developed at surface 4 and incised valleys at surfaces 2 and 4 suggest base-level lowering of as much as 50 to 60 m. Base-level lowering of < 50 m is also possible, although inferred with less confidence, at surface 5. A glacio-eustatic origin is permitted for each of these surfaces, although not required. Available evidence does not support marked sea-level changes at other horizons. The mismatch between carbon isotope minima and sequence boundaries in the Infra Krol–Krol succession suggests that such isotopic minima in the Neoproterozoic do not necessarily correlate with times of glaciation, and that ice sheets of modest scale (comparable to those of the Oligocene or the present) may have existed during apparently nonglacial times without producing either cap carbonates or negative carbon isotope excursions.

ACKNOWLEDGMENTS

The research reported here grew out of a field workshop sponsored by the Palaeontological Society of India and International Geological Correlation Programme Project 303 in Dehradun in January, 1994. The authors thank the many participants of that conference for insights on the regional stratigraphy, paleontology, and sedimentology of the Lesser Himalaya. We are especially grateful to R. Shanker (Geological Survey of India), I.B. Singh and S. Kumar (Lucknow University), V.C. Tewari (Wadia Institute), and O.P. Goel and S.B. Misra (Kumun University) for stimulating discussions, and for advice about sections suitable for this study. We are indebted also to H. Kumar (Dehradun) and B. Nath (University of Delhi) for logistical and linguistic assistance to GJ in the field, and to K. Miller at Empress Travel in Lawrenceville, New Jersey, for heroic intervention when Jiang became ensnared by consular and airline bureaucracy in Delhi. We are grateful to A.H. Knoll, P.M. Myrow, B.R. Pratt, R. Shanker, and S. Xiao; to journal reviewers M.R. Saltzman and K.A. Giles; and to B.H. Wilkinson (associate editor) and D.A. Budd (editor) for their constructive comments and advice. The research was supported by National Science Foundation Grant EAR 96–14070. Lamont-Doherty Earth Observatory Contribution Number 6291.

REFERENCES

Aharon, P., Schidlowski, M., and Singh, I.B., 1987, Chronostratigraphic markers in the end-Precambrian carbon isotope record of the Lesser Himalaya: Nature, v. 327, p. 699–702.

Auden, J.B., 1934, The geology of the Krol belt: Geological Survey of India Record, v. 71, p. 357–454.

Azmi, R.J., 1983, Microfauna and age of Lower Tal phosphorite of Mussoorie syncline, Garhwal Lesser Himalaya: Himalayan Geology, v. 11, p. 373–409.

Azmi, R.J., and Pancholi, V.P., 1983, Early Cambrian (Tommotian) conodonts and other shelly microfauna from the Upper Krol of Mussoorie Syncline, Garhwal Lesser Himalaya, with remarks on Precambrian–Cambrian boundary: Himalayan Geology, v. 11, p. 360–372.

Banerjee, D.M., Schidlowski, M., Siebert, F., and Brasier, M.D., 1997, Geochemical changes across the Precambrian–Cambrian transition in the Durmala phosphorite mine section, Mussoorie Hills, Garhwal Himalaya, India: Palaeogeography, Palaeoclimatology, Palaeoecology, v. 132, p. 183–194.

Beach, D.K., 1995, Controls and effects of subaerial exposure on cementation and development of secondary porosity in the subsurface of Great Bahama Bank, *in* Budd, D.A., Saller, A.H., and Harris, P.M., eds., Unconformities and Porosity in Carbonate Strata: American Association of Petroleum Geologists, Memoir 63, p. 1–34.

Beukes, N.J., 1987, Facies relations, depositional environments and diagenesis in a major Proterozoic stromatolitic carbonate platform to basinal sequence, Campbellrand Supergroup, Transvaal Supergroup, southern Africa: Sedimentary Geology, v. 54, p. 1–46.

Bhargava, A.K., and Singh, I.B., 1981, Some paleoenvironmental observations on the Infra Krol Formation, Lesser Himalaya: Palaeontological Society of India, Journal, v. 25, p. 26–32.

Bhargava, O.N., 1979, Lithostratigraphic classification of the Blaini, Infra-Krol, Krol and Tal formations: a review: Geological Society of India, Journal, v. 20, p. 7–16.

Bhatia, M.R., and Prasad, A.K., 1975, Some sedimentological, lithostratigraphic and genetic aspects of the Blaini Formation of parts of Simla Hills, Himachal Pradesh, India: Indian Geological Association, Bulletin, v. 8, p. 162–185.

Bhatt, D.K., 1989, Small shelly fossils, Tommotian and Meishucunian stages and the Precambrian–Cambrian boundary—implications of the recent studies in the Himalayan sequences: Palaeontological Society of India, Journal, v. 34, p. 55–68.

Bhatt, D.K., 1991, The Precambrian–Cambrian transition interval in Himalaya with special reference to small shelly fossils—A review of current status of work: Palaeontological Society of India, Journal, v. 36, p. 109–120.

Bhatt, D.K., 1996, The end phase of sedimentation of Krol Belt succession in Nainital syncline—stratigraphic analysis and fossil levels: Current Science, v. 70, p. 772–774.

Bhatt, D.K., Mamgain, A.K., and Misra, R.S., 1985, Small shelly fossils of Early Cambrian (Tommotian) age from Chert–Phosphorite Member, Tal Formation, Mussoorie syncline, Lesser Himalaya, India and their chronostratigraphic evaluation: Paleontological Society of India, Journal, v. 30, p. 92–102.

Bhattacharyya, A., and Chanda, S.K., 1971, Petrology and origin of the Krol Sandstone around Solan, Himachal Pradesh: Geological Society of India, Journal, v. 12, p. 368–374.

Bhattacharya, S.C., and Niyogi, D., 1971, Geological evolution of the Krol Belt in Simla Hills, H.P.: Himalayan Geology, v. 1, p. 178–212.

Bosák, P., Ford, D.C., Głazek, J., and Horáček, I., eds., 1989, Paleokarst: A systematic and regional review: Amsterdam, Elsevier Science Publishing Company, p. 16–34, and p. 565–598.

Bowring, S.A., and Erwin, D.H., 1998, A new look at evolutionary rates in deep time: Uniting paleontology and high-precision geochronology: GSA Today, v. 8, p. 1–8.

Brasier, M.D., and Singh, P., 1987, Microfossils and Precambrian–Cambrian boundary stratigraphy at Maldeota, Lesser Himalaya: Geological Magazine, v. 124, p. 323–345.

Brookfield, M.E., 1993, The Himalayan passive margin from Precambrian to Cretaceous times: Sedimentary Geology, v. 84, p. 1–35.

Budd, D.A., Hammes, U., and Vacher, H.L., 1993, Calcite cementation in the upper Floridan aquifer: a modern example for confined-aquifer cementation models?: Geology, v. 21, p. 33–36.

Cander, H., 1995, Interplay of water–rock interaction efficiency, unconformities, and fluid flow in a carbonate aquifer: Floridan aquifer system, *in* Budd, D.A., Saller, A.H., and Harris, P.M., eds., Unconformities and Porosity in Carbonate Strata: American Association of Petroleum Geologists, Memoir 63, p. 103–124.

Choquette, P.W., and James, N.P., 1988, Introduction, *in* James, N.P., and Choquette, P.W., eds., Paleokarst: New York, Springer-Verlag, p. 1–21.

Christie-Blick, N., 1997, Neoproterozoic sedimentation and tectonics in west-central Utah, *in* Link, P.K., and Kowallis, B.J., eds., Proterozoic to Recent Stratigraphy, Tectonics and Volcanology, Utah, Nevada, Southern Idaho and Central Mexico: Brigham Young University Geology Studies, v. 42, Part I, p. 1–30.

Christie-Blick, N., and Driscoll, N.W., 1995, Sequence stratigraphy: Annual Review of Earth and Planetary Sciences, v. 23, p. 451–478.

CHRISTIE-BLICK, N., DYSON, I.A., AND VON DER BORCH, C.C., 1995, Sequence stratigraphy and the interpretation of Neoproterozoic earth history: Precambrian Research, v. 73, p. 3–26.

CHRISTIE-BLICK, N., SOHL, L.E., AND KENNEDY, M.J., 1999, Considering a Neoproterozoic snowball Earth (technical comment): Science, v. 284, p. 1087.

CROWELL, J.C., 1999, Pre-Mesozoic Ice Ages: Their Bearing on Understanding the Climate System: Geological Society of America, Memoir 192, 106 p.

CVIJIC, J., 1981, The dolines, *in* Sweeting, M.M., ed., Karst Geomorphology: Stroudsburg, Pennsylvania, Hutchinson Ross Publishing Company, Benchmark Papers in Geology, v. 59, p. 23–41.

DECELLES, P.G., GEHRELS, G.E., QUADE, J., LAREAU, B., AND SPURLIN, M., 2000, Tectonic implications of U–Pb zircon ages of the Himalayan orogenic belt in Nepal: Science, v. 288, p. 497–499.

DESROCHERS, A., AND JAMES, N.P., 1988, Early Paleozoic surface and subsurface paleokarst in Middle Ordovician carbonates, Mingan Islands, Quebec, *in* James, N.P., and Choquette, P.W., eds., Paleokarst: New York, Springer-Verlag, p. 183–210.

EVANS, D.A.D., 2000, Stratigraphic, geochronological, and paleomagnetic constraints upon the Neoproterozoic climatic paradox: American Journal of Science, v. 300, p. 347–433.

FAIRBANKS, R.G., 1989, A 17,000-year glacio-eustatic sea level record: influence of glacial melting rates on the Younger Dryas event and deep-ocean circulation: Nature, v. 342, p. 637–642.

GARZANTI, E., CASNEDI, R., AND JADOUL, F., 1986, Sedimentary evidence of a Cambro–Ordovician orogenic event in the northwestern Himalaya: Sedimentary Geology, v. 48, p. 237–265.

GAUTAM, R., AND RAI, V., 1997, Branched microbiota from the bedded black chert of the Krol Formation (Neoproterozoic), Lesser Himalaya, India: Palaeobotanist, v. 46, p. 32–40.

GROTZINGER, J.P., 1986a, Cyclicity and paleoenvironmental dynamics, Rocknest platform, northwest Canada: Geological Society of America, Bulletin, v. 97, p. 1208–1231.

GROTZINGER, J.P., 1986b, Evolution of Early Proterozoic passive-margin carbonate platform, Rocknest Formation, Wopmay Orogen, Northwest Territories, Canada: Journal of Sedimentary Petrology, v. 56, p. 831–847.

GROTZINGER, J.P., 1989, Construction of early Proterozoic (1.9 Ga) barrier reef complex, Rocknest Platform, Northwest Territories, *in* Geldsetzer, H.H.J., James, N.P., and Tebbut, G.E., eds., Reefs, Canada and Adjacent Areas: Canadian Society of Petroleum Geologists, Memoir 13, p. 30–37.

GROTZINGER, J.P., BOWRING, S.A., SAYLOR, B.Z., AND KAUFMAN, A.J., 1995, Biostratigraphic and geochronologic constraints on early animal evolution: Science, v. 270, p. 598–604.

GUPTA, V.J., AND KANWAR, R.C., 1981, Late Paleozoic diamictites of the Kashmir Tethys and Himachal Pradesh Himalaya, India, *in* Hambrey, M.J., and Harland, W.B., eds., Earth's Pre-Pleistocene Glacial Record: Cambridge, U.K., Cambridge University Press, p. 287–293.

HANDFORD, C.R., AND LOUCKS, R.G., 1993, Carbonate depositional sequences and systems tracts—Responses of carbonate platforms to relative sea-level changes, *in* Loucks, R.G., and Sarg, J.F., eds., Carbonate Sequence Stratigraphy: American Association of Petroleum Geologists, Memoir 57, p. 1–41.

HARLAND, W.B., 1964, Critical evidence for a great Infracambrian glaciation: Geologische Rundschau, v. 54, p. 45–61.

HODGES, K.V., 2000, Tectonics of the Himalaya and southern Tibet from two perspectives: Geological Society of America, Bulletin, v. 112, p. 324–350.

HOFFMAN, P.F., KAUFMAN, A.J., HALVERSON, G.P., AND SCHRAG, D.P., 1998, A Neoproterozoic snowball earth: Science, v. 281, p. 1342–1346.

JACOBSEN, S.B., AND KAUFMAN, A.J., 1999, The Sr, C, and O isotopic evolution of Neoproterozoic seawater: Chemical Geology, v. 161, p. 37–57.

JAMES, N.P., AND CHOQUETTE, P.W., 1984, Diagenesis 9: limestones—the meteoric diagenetic environment: Geoscience Canada, v. 11, p. 161–194.

JENNINGS, J.N., 1985, Karst Geomorphology: Oxford, U.K., Blackwell Scientific Publications, 293 p.

JIANG, G., 2002, Neoproterozoic sequence and chemostratigraphy [unpublished Ph.D. dissertation]: New York, Columbia University, 227 p.

JOECKEL, R.M., 1999, Paleosol in Galesburg Formation (Kansas City Group, Upper Pennsylvanian), northern Midcontinent, U.S.A.: Evidence for climate change and mechanisms of marine transgression: Journal of Sedimentary Research, v. 69, p. 720–737.

KAHLE, C.F., 1988, Surface and subsurface paleokarst, Silurian Lockport, and Peebles Dolomites, Western Ohio, *in* James, N.P., and Choquette, P.W., eds., Paleokarst: New York, Springer-Verlag, p. 229–255.

KAUFMAN, A.J., AND KNOLL, A.H., 1995, Neoproterozoic variations in C isotopic composition of seawater: Stratigraphic and biogeochemical implications: Precambrian Research, v. 73, p. 27–50.

KAUFMAN, A.J., KNOLL, A.H., AND NARBONNE, G.M., 1997, Isotopes, ice ages, and terminal Proterozoic earth history: National Academy of Sciences, Proceedings, v. 94, p. 6600–6605.

KENNEDY, M.J., 1996, Stratigraphy, sedimentology, and isotopic geochemistry of Australian Neoproterozoic postglacial dolostones: Deglaciation, $\delta^{13}C$ excursions, and carbonate precipitation: Journal of Sedimentary Research, v. 66, p. 1050–1064.

KENNEDY, M.J., RUNNEGAR, B., PRAVE, A.R., HOFFMANN, K.-H., AND ARTHUR, M.A., 1998, Two or four Neoproterozoic glaciations?: Geology, v. 26, p. 1059–1063.

KERANS, C., AND DONALDSON, J.A., 1988, Proterozoic paleokarst profile, Dismal Lakes Group, N.W.T., Canada, *in* James, N.P., and Choquette, P.W., eds., Paleokarst: New York, Springer-Verlag, p. 167–182.

KIRSCHVINK, J.L., 1992, Late Proterozoic low-latitude global glaciation: the snowball Earth, *in* Schopf, J.W., and Klein, C., eds., The Proterozoic Biosphere: A Multidisciplinary Study: Cambridge, U.K., Cambridge University Press, p. 51–52.

KNOLL, A.H., 2000, Learning to tell Neoproterozoic time: Precambrian Geology, v. 100, p. 3–20.

KNOLL, A.H., AND WALTER, M.R., 1992, Latest Proterozoic stratigraphy and earth history: Nature, v. 356, p. 673–678.

KNOLL, A.H., KAUFMAN, A.J., SEMIKHATOV, M.A., GROTZINGER, J.P., AND ADAMS, W., 1995, Sizing up the sub-Tommotian unconformity in Siberia: Geology, v. 23, p. 1139–1143.

KNOLL, A.H., KAUFMAN, A.J., SWETT, K., AND LAMBERT, I.B., 1986, Secular variation in carbon isotope ratios from the upper Proterozoic succession of Svalbard and east Greenland: Nature, v. 321, p. 832–839.

KOMINZ, M.A., AND PEKAR, S.F., 2001, Oligocene eustasy from two-dimensional sequence stratigraphic backstripping: Geological Society of America, Bulletin, v. 113, p. 291–304.

KUMAR, G., BHATT, D.K., AND RAINA, B.K., 1987, Skeletal microfauna of Meishucunian and Qiongzhusian (Precambrian–Cambrian boundary) age from the Ganga Valley, Lesser Himalaya, India: Geological Magazine, v. 124, p. 167–171.

KUMAR, R., AND BROOKFIELD, M.E., 1987, Sedimentary environments of the Simla Group (Upper Precambrian), Lesser Himalaya, and their paleotectonic significance: Sedimentary Geology, v. 52, p. 27–43.

KUMAR, S., AND RAI, V., 1992, Organic-walled microfossils from the bedded black chert of the Krol Formation (Vendian), Solan area, Himachal Pradesh, India: Geological Society of India, Journal, v. 39, p. 229–234.

LE FORT, P., DEBON, F., AND SONET, J., 1983, The lower Paleozoic 'Lesser Himalaya' granitic belt: emphasis on the Simchar pluton of Center Nepal, *in* Shams, F.A., ed., Granites of Himalayas, Karakorum and Hindu Kush: Lahore, Punjab University, p. 235–253.

LEVY, M., CHRISTIE-BLICK, N., AND LINK, P.K., 1994, Neoproterozoic incised valleys of the eastern Great Basin, Utah and Idaho: Fluvial response to changes in depositional base level, *in* Dalrymple, R., Boyd, R., and Zaitlin, B., eds., Incised Valley Systems: Origin and Sedimentary Sequences: SEPM, Special Publication 51, p. 369–382.

LUCIA, F.J., 1995, Lower Paleozoic cave development, collapse, and dolomitization, Franklin Mountains, El Paso, Texas, *in* Budd, D.A., Saller, A.H., and Harris, P.M., eds., Unconformities and Porosity in Carbonate Strata: American Association of Petroleum Geologists, Memoir 63, p. 279–300.

MASLYN, R.M., 1977, Fossil tower karst near Molas Lake, Colorado: Mountain Geology, v. 14, p. 17–25.

MATHUR, V.K., 1989, Biostratigraphic studies in the Krol Belt, Lesser Himalaya: Geological Survey of India, Record, v. 122, p. 233–235.

MATHUR, V.K., AND SHANKER, R., 1989, First record of Ediacaran fossils from the Krol Formation, Nainital syncline: Geological Society of India, Journal, v. 34, p. 245–254.

MATHUR, V.K., AND SHANKER, R., 1990, Ediacaran medusoids from Cambrian Tal Formation, Himachal Lesser Himalaya and the Krol Formation, Naini Tal syncline: Geological Society of India, Journal, v. 36, p. 74–78.

MISRA, S.B., 1984, Depositional environment of the Krol Group of the Nainital area and its impact on the stromatolites: Indian Academy of Science, Proceedings (Earth and Planetary Science), v. 93, p. 447–464.

MISRA, S.B., 1990, Comment on the paper ''First record of Ediacaran fossils from the Krol Formation of Nainital syncline'': Geological Society of India, Journal, v. 35, p. 114–115.

MISRA, S.B., 1992, On the occurrence of Ediacarian (?) dubiofossils in the Narainnagar Formation of Nainital area, U.P., India: Geological Society of India, Journal, v. 39, p. 401–409.

MUSTARD, P.S., AND DONALDSON, J.A., 1990, Paleokarst breccias, calcretes, silcretes and fault breccias at the base of Upper Proterozoic ''Windermere'' strata, northern Canadian Cordillera: Journal of Sedimentary Petrology, v. 60, p. 525–539.

MYLROIE, J.E., AND CAREW, J.L., 1995, Karst development on carbonate islands, *in* Budd, D.A., Saller, A.H., and Harris, P.M., eds., Unconformities and Porosity in Carbonate Strata: American Association of Petroleum Geologists, Memoir 63, p. 55–76.

NARBONNE, G.M., KAUFMAN, A.J., AND KNOLL, A.H., 1994, Integrated chemostratigraphy and biostratigraphy of the upper Windermere Group (Neoproterozoic), Mackenzie Mountains, northwestern Canada: Geological Society of America, Bulletin, v. 106, p. 1281–1292.

PALMER, A.N., 1991, Origin and morphology of limestone caves: Geological Society of America, Bulletin, v. 103, p. 1–21.

PALMER, A.N., 1995, Geochemical models for the origin of macroscopic solution porosity in carbonate rocks, *in* Budd, D.A., Saller, A.H., and Harris, P.M., eds., Unconformities and Porosity in Carbonate Strata: American Association of Petroleum Geologists, Memoir 63, p. 77–102.

PELECHATY, S.M., AND JAMES, N.P., 1991, Dolomitized Middle Proterozoic calcretes, Bathurst Inlet, northwest Territories, Canada: Journal of Sedimentary Petrology, v. 61, p. 988–1001.

PELECHATY, S.M., GROTZINGER, J.P., KASHIRTSEV, V.A., AND ZHERNOVSKY, V.P., 1996, Chemostratigraphic and sequence stratigraphic constraints on Vendian–Cambrian basin dynamics, northeast Siberian craton: Journal of Geology, v. 104, p. 543–564.

PELECHATY, S.M., JAMES, N.P., KERANS, C., AND GROTZINGER, J.P., 1991, A middle Proterozoic paleokarst unconformity and associated sedimentary rocks, Elu Basin, northwest Canada: Sedimentology, v. 38, p. 775–797.

PLINT, A.G., HART, B.S., AND DONALDSON, W.S., 1993, Lithospheric flexure as a control on stratal geometry and facies distribution in Upper Cretaceous rocks of the Alberta foreland basin: Basin Research, v. 5, p. 69–77.

POSAMENTIER, H.W., AND JAMES, D.P., 1993, An overview of sequence-stratigraphic concepts: uses and abuses, *in* Posamentier, H.W., Summerhayes, C.P., Haq, B.U., and Allen, G.P., eds., Sequence Stratigraphy and Facies Associations: International Association of Sedimentologists, Special Publication 18, p. 3–18.

POWERS, P.M., LILLIE, R.J., AND YEATS, R.S., 1998, Structure and shortening of the Kangra and Dehra Dun re-entrants, Sub-Himalaya, India: Geological Society of America, Bulletin, v. 110, p. 1010–1027.

RAI, V., AND SINGH, I.B., 1983, Discovery of trilobite impression in the Arenaceous Member of Tal Formation, Mussoorie area, India: Palaeontological Society of India, Journal, v. 28, p. 114–117.

READ, J.F., 1995, Overview of carbonate platform sequences, cycle stratigraphy and reservoirs in greenhouse and ice-house worlds, *in* Read, J.F., Kerans, C., Weber, L.J., Sarg, J.F., and

Wright, F.M., eds., Milankovitch Sea-Level Changes, Cycles, and Reservoirs on Carbonate Platforms in Greenhouse and Ice-House Worlds: SEPM, Short Course 35, Part 1, p. 1–102.

ROSSETTI, D.D.F., 1998, Facies architecture and sequential evolution of an incised-valley estuarine fill: the Cujupe Formation (Upper Cretaceous to? Lower Tertiary), Sao Luis Basin, northern Brazil: Journal of Sedimentary Research, v. 68, p. 299–310.

SAMI, T.T., AND JAMES, N.P., 1993, Evolution of an early Proterozoic foreland basin carbonate platform, lower Pethei Group, Great Slave Lake, north-west Canada: Sedimentology, v. 40, p. 403–430.

SAMI, T.T., AND JAMES, N.P., 1994, Peritidal carbonate platform growth and cyclicity in an early Proterozoic foreland basin, Upper Pethei Group, northwest Canada: Journal of Sedimentary Research, v. B64, p. 111–131.

SARG, J.F., 1988, Carbonate sequence stratigraphy, *in* Wilgus, C.K., Hastings, B.S., Kendall, C.G.St.C., Posamentier, H.W., Ross, C.A., and van Wagoner, J.C., eds., Sea-Level Changes: An Integrated Approach: SEPM, Special Publication 42, p. 155–181.

SAYLOR, B.Z., KAUFMAN, A.J., GROTZINGER, J.P., AND URBAN, F., 1998, The partitioning of terminal Proterozoic time: Constraints from Namibia: Journal of Sedimentary Research, v. 68, p. 1223–1235.

SHANKER, R., AND MATHUR, V.K., 1992, Precambrian–Cambrian sequence in Krol Belt and additional Ediacaran fossils: Geophytology, v. 22, p. 27–39.

SHANKER, R., KUMAR, G., AND SAXENA, S.P., 1989, Stratigraphy and sedimentation in Himalaya, a reappraisal: Geological Survey of India, Special Publication 26, p. 1–60.

SHANKER, R., KUMAR, G., MATHUR, V.K., AND JOHSI, A., 1993, Stratigraphy of Blaini, Infra Krol and Tal succession, Krol Belt, Lesser Himalaya: Indian Journal of Petroleum Geology, v. 2, p. 99–136.

SHANKER, R., MATHUR, V.K., KUMAR, G., AND SRIVASTAVA, M.C., 1997, Additional Ediacaran biota from the Krol Group, Lesser Himalaya, India and their significance: Geoscience Journal, v. 18, p. 79–91.

SINGH, I.B., 1980a, Sedimentological evolution of the Krol Belt sediments: Himalayan Geology, v. 8, p. 657–683.

SINGH, I.B., 1980b, Precambrian sedimentary sequences of India: their peculiarities and comparison with modern sediments: Precambrian Research, v. 12, p. 411–436.

SINGH, I.B., 1981, A critical review of the fossil records in the Krol Belt succession and its implications on the biostratigraphy and paleogeography of the Lesser Himalaya: Palaeontological Society of India, Journal, v. 25, p. 148–169.

SINGH, I. B., AND RAI, V., 1977, On occurrence of stromatolites in the Krol Formation of Nainital area and its implications on the age of Krol Formation: Current Science, v. 46, p. 736–738.

SINGH, I.B., AND RAI, V., 1980, Some observations on the depositional environment of the Krol Formation in Nainital area: Himalayan Geology, v. 8, p. 633–656.

SINGH, I.B., AND RAI, V., 1983, Fauna and biogenic structures in Krol–Tal succession (Vendian–Early Cambrian), Lesser Himalaya and a biostratigraphic and palaeontological significance: Palaeontological Society of India, Journal, v. 28, p. 67–90.

SINGH, I.B., RAI, V., AND BHARGAVA, A.K., 1980, Some observations on the sedimentology of the Krol succession of Mussoorie area, Uttar Pradesh: Geological Society of India, Journal, v. 21, p. 232–238.

SMITH, M.P., SOPER, N.J., HIGGINS, A.K., RASMUSSEN, J.A., AND CRAIG, L.E., 1999, Paleokarst systems in the Neoproterozoic of eastern North Greenland in relation to extensional tectonics on the Laurentian margin: Geological Society of London, Journal, v. 156, p. 113–124.

SOHL, L.E., CHRISTIE-BLICK, N., AND KENT, D.V., 1999, Paleomagnetic polarity reversals in Marinoan (~ 600 Ma) glacial deposits of Australia: Implications for the duration of low-latitude glaciation in Neoproterozoic time: Geological Society of America, Bulletin, v. 111, p. 1120–1139.

TALLING, P.J., 1998, How and where do incised valleys form if sea level remains above the shelf edge?: Geology, v. 26, p. 87–90.

TEWARI, V.C., 1993a, Ediacarian metaphytes from the lower Krol Formation, Lesser Himalaya: Geoscience Journal, v. 14, p. 145–148.

TEWARI, V.C., 1993b, Precambrian and Lower Cambrian stromatolites of the lesser Himalaya, India: Geophytology, v. 23, p. 19–39.

TEWARI, V.C., AND JOSHI, M., 1993, Stromatolite microstructures: a new tool for biostratigraphic correlation of Lesser Himalayan carbonates: Journal of Himalayan Geology, v. 4, p. 171–181.

TINKER, S.W., EHRETS, J.R., AND BRONDOS, M.D., 1995, Multiple karst events related to stratigraphic cyclicity: San Andres Formation, Yates Field, West Texas, *in* Budd, D.A., Saller, A.H., and Harris, P.M., eds., Unconformities and Porosity in Carbonate Strata: American Association of Petroleum Geologists, Memoir 63, p. 213–238.

TIWARI, M., 1999, Organic-walled microfossils from the Chert–phosphorite Member, Tal Formation, Precambrian–Cambrian Boundary, India: Precambrian Geology, v. 99, p. 99–113.

TIWARI, M., AND KNOLL, A.H., 1994, Large acanthomorphic Acritarchs from the Infrakrol Formation of the Lesser Himalaya and their stratigraphic significance: Journal of Himalayan Geology, v. 5, p. 193–201.

VAIL, P.R., 1987, Seismic stratigraphy interpretation using sequence stratigraphy. Part 1: Seismic stratigraphy interpretation procedure, *in* Bally, A.W., ed., Atlas of Seismic Stratigraphy: American Association of Petroleum Geologists, Studies in Geology No. 27, v. 1, p. 1–10.

VALDIYA, K.S., 1992, The Main Boundary thrust zone of the Himalaya, India: Annales Tectonicae, v. 6, p. 54–84.

VAN WAGONER, J.C., MITCHUM, R.M., CAMPION, K.M., AND RAHMANIAN, V.D., 1990, Siliciclastic Sequence Stratigraphy in Well Logs, Cores, and Outcrops: Concepts for High-Resolution Correlation of Time and Facies: American Association of Petroleum Geologists Methods in Exploration Series, No. 7, 55 p.

VANSTONE, S.D., 1991, Early Carboniferous (Mississippian) paleosols from southwest Britain: Influence of climatic change on soil development: Journal of Sedimentary Petrology, v. 61, p. 445–457.

VANSTONE, S.D., 1998, Late Dinantian paleokarst of England and Wales: implications for exposure surface development: Sedimentology, v. 45, p. 19–37.

WAGNER, P.D., TASKER, D.R., AND WAHLMAN, G.P., 1995, Reservoir degradation and compartmentalization below subaerial unconformities: limestone examples from west Texas, China, and Oman, *in* Budd, D.A., Saller, A.H., and Harris, P.M., eds., Unconformities and Porosity in Carbonate Strata: American Association of Petroleum Geologists, Memoir 63, p. 177–196.

WOOLFE, K.J., LARCOMBE, P., NAISH, T., AND PURDON, R.G., 1998, Lowstand rivers need not incise the shelf: An example from the Great Barrier Reef, Australia, with implications for sequence stratigraphic models: Geology, v. 26, p. 75–78.

WRIGHT, V.P., 1982, The recognition and interpretation of paleokarsts: two examples from the Lower Carboniferous of south Wales: Journal of Sedimentary Petrology, v. 52, p. 83–94.

WRIGHT, V.P., 1994, Paleosols in shallow marine carbonate sequences: Earth-Science Reviews, v. 35, v. 367–395.

XIAO, S., ZHANG, Y., AND KNOLL, A.H., 1998, Three-dimensional preservation of algae and animal embryos in a Neoproterozoic phosphorite: Nature, v. 391, p. 553–558.

YANG, K.M., AND DOROBEK, S.L., 1995, The Permian basin of west Texas and New Mexico: tectonic history of a ''composite'' foreland basin and its effects on stratigraphic development, *in* Dorobek, S.L., and Ross, G.M., eds., Stratigraphic Evolution of Foreland Basins: SEPM, Special Publication 52, p. 37–52.

ZAITLIN, B.A., DALRYMPLE, R.W., AND BOYD, R., 1994, The stratigraphic organization of incised-valley systems associated with relative sea-level change, *in* Dalrymple, R., Boyd, R., and Zaitlin, B., eds., Incised Valley Systems: Origin and Sedimentary Sequences: SEPM, Special Publication 51, p. 45–60.

Received 28 July 2000; accepted 3 December 2001.